SAMPLE REPORT

THE CONCUSSION GROUP

Let's talk about your mTBI case.

www.theconcussiongroup.com
888.214.2095

Neuroscientific Report on
Quantitative MRI Volumetrics and Diffusion Tensor Imaging

Client: [redacted]
DOB: [redacted]
Gender: Male
Date of Exam: 02/24/2020
Date of Report: 03/05/2020
Report By: Jeffrey David Lewine, Ph.D.

Background (from self-report notes):

[redacted] is a 34-year-old male who reports suffering a head trauma during a motor vehicle accident in February of 2018. He does not know if he suffered a loss-of-consciousness. Although he does not explicitly report any prior head traumas he indicates a sports history that includes football, basketball, and baseball. Currently he self-reports numerous post-concussive symptoms including headaches, confusion, slurred speech, behavioral changes, depression, fatigue, sleeplessness, and memory problems.

Technical Details:

Magnetic Resonance Imaging data were collected at an MRN scanner partnered with The Concussion Group. Data were collected using a Siemens 3.0 Tesla TRIO system. Employed imaging sequences included a T1-weighted 3D volumetric acquisition, T2 and FLAIR sequences, susceptibility weighted imaging (SWI) and diffusion tensor imaging
(DTI).

Quantitative volumetric and DTI analyses were performed by Dr. Jeffrey David Lewine, Ph.D. and his colleagues at the MINDSET Consulting Group in Albuquerque, NM. Dr. Lewine is a neuroscientist. All opinions reported herein are from a neuroscientific perspective. After completing volumetric and DTI analyses (using appropriate analytic pipelines and statistical methods as described below), Dr. Lewine generated this report and forwarded it, in its entirety, to the Concussion Group for final transmission to the referring medical care providers through the MRN scanner.

Images from the thin-slice, T1-weighted 3D acquisition were used for quantitative volumetric analyses. Dr. Lewine and his team utilized a standardized, objective, and automated SPM12-based processing pipeline to calculate regional brain volumes for 107 brain areas pre-selected from TD-Brodmann and AAL Atlases. These volumetric measures were then scaled by total intracranial volume to correct for head size. As part of the

analysis process, data were assessed for motion and other artifacts that might substantially compromise the validity of results. The volumetric data for Mr. [redacted] were found to be of acceptable quality for viable interpretation.

Data from the Diffusion Tensor Imaging sequence were used for quantitative evaluation of white matter integrity, with regional Fractional Anisotropy (FA) as the core metric. Standardized, objective, and automated FSL-based procedures were used to calculate FA values from 48 fiber tract regions pre-selected from the Johns Hopkins University white matter atlas. As part of the analysis process, data were assessed for motion and other artifacts that might substantially compromise the validity of results. The DTI data for Mr. [redacted] were found to be of acceptable quality for viable interpretation.

Volumetric and FA metrics for Mr. [redacted] were statistically evaluated with respect to average volumetric and FA metrics derived from all gender and age-range (+/- 10 years) matched control subjects within a large database of >1000 neuro-typical subjects that is maintained by MINDSET. The MINDSET control data had been collected on a MRI system that belongs to the Mind Research Network (MRN) in Albuquerque. The Concussion Group (TCG) MRN scanners are of the same type (3.0 T TIM-TRIO) and same manufacturer (Siemens). The data acquisition parameters for Mr. [redacted] were set to be identical to those used by all TCG MRN scanners in the collection of the control datasets. The data analysis software algorithms, procedures, and processing pipeline used to assess data from Mr. [redacted] and the MRN control subjects were identical. Prior to statistical analyses, data metrics from Mr. [redacted] were scaled using region-specific factors derived from a traveling human phantom previously evaluated on all TCG MRN scanners. These factors provide for harmonization of TCG MRN datasets and allow Mr. [redacted]'s data to be validly evaluated with respect to the MINDSET normative database. The MINDSET database was created by pooling control subjects across 36 IRB-approved studies at MRN. For membership in the neuro-typical control group of each study, a reported history of traumatic brain injury, or report of a diagnosed neurological or psychiatric disease or injury, substance use disorder, learning disability, or developmental disability was exclusionary. For the statistical evaluation of the TCG data from Mr. [redacted], a total of **161** matched MINDSET control datasets were identified for volumetric evaluation, with **161** datasets identified for FA evaluation.

The appendix document TCG-Appendix-I-MRI provides a brief overview of basic neurobiology, conceptual and technical details on MRI volumetric and diffusion tensor imaging procedures, and how this information is used in the forensic evaluation of traumatic brain injury cases.

Volumetric Findings:

As shown in Figure 1, volumetric analyses conducted individually on 107 brain regions for Mr. [redacted] showed **18 of the 107** regions to have atypical volumes (**p<0.05; 8 low; 10 high**). Given the number of multiple comparisons (N=107), there is an expectation that even a subject without any history of neurological/psychiatric disease or injury will show a handful of brain regions with 'false positive' identification as abnormal. To address this issue of false positives during multiple comparisons, a Benjamini-Hochberg correction was applied with a False Discovery Rate of 25%. Following this correction, **only 11** of the

brain regions with atypical volume on isolated individual evaluation are still considered to be abnormal from a statistical perspective **(5 low; 6 high)**. Figure 2 provides a spatial display of the brain regions with abnormal volumes at the level of individual testing. Table 1 provides a description of the functions of evaluated brain regions. An * in Figure 1 and Table 1 indicates a brain region with a statistically abnormal volume, even after correction for multiple comparisons.

Diffusion Tensor Imaging Findings

As shown in Figure 3, DTI analyses conducted individually on 48 fiber tract regions for Mr. [redacted] showed **10 of the 48** tract regions to have atypical FA values (**p<0.05; 0 low; 10 high**). Given the number of multiple comparisons (N=48), there is an expectation that some tracts may be falsely identified as abnormal even for neurotypical subjects. To address this issue, the data were additionally evaluated using a Benjamini-Hochberg correction for multiple comparisons, with a false discovery rate of 25%. Following this correction, **ALL 10** of the fiber tract regions that showed atypical FA values on isolated individual evaluation are still considered to show abnormal FA values from a statistical perspective **(0 low; 10 high)**.

Table 2 provides information on the statistical evaluation of each individual tract. Scatter plots showing the data from Mr. [redacted] with respect to **583** neurotypical male subjects in the MRN database are provided in the appendix document: TCG-Appendix-II-Scatter-Plots-[redacted]. Table 3 summarizes connectivity and functional information on the various fiber tract regions. Additional information on the various fiber tracts is provided in the appendix document: TCG-Appendix-I-MRI**.** An * in Figure 3 and Table 2 indicates a fiber tract region with a statistically abnormal FA value, even after correction for multiple comparisons.

Neuroscientific Impressions:

Volumetric data for Mr. [redacted] were abnormal.

After correction for multiple comparisons, the data indicated that **11 of the 107** evaluated brain regions showed abnormal volumes from a purely statistical perspective **(5 low; 6 high)**. Low volumes may reflect perturbation of early developmental processes, malnutrition, toxic stress, toxic exposures, or more commonly neurological-psychiatric disease and/or brain injury. High volumes may reflect a perturbation of early developmental processes, baseline skill enhancement, edema, astrogliosis, chronic inflammation or reactive compensatory mechanisms in relationship to compromise of other brain regions. Following head trauma, both abnormally low and abnormally high regional brain values have been reported in the peer-reviewed scientific literature.

Mr. [redacted] showed statistically low volumes in 5 brain regions. Regions with low volume included bilateral orbital frontal areas. The orbital frontal is involved in the emotional regulation of behavior and other executive functions and is known to be especially vulnerable to traumatic forces.

Mr. [redacted] showed statistically high volumes in 6 brain regions. High volumes were seen scattered throughout the brain, but included the corpus callosum which is known to be especially vulnerable to traumatic forces. Regions with high volumes normally support interhemispheric integration, memory, olfaction, and motor control.

DTI data for Mr. [redacted] were abnormal.

After correction for multiple comparisons, the data indicated that **10 of the 48** evaluated fiber tract regions showed abnormal FA values from a purely statistical perspective **(10 low; 0 high)**. Possible causes for high FA include a developmental failure of axonal pruning, disease/injury related intracellular cytogenic edema, compaction of neurofilament, neuro-inflammation with microglial activation, astrogliosis, loss of crossing fibers, and/or compensatory mechanisms. Following head trauma, both abnormally low and abnormally high FA values have been reported in the peer-reviewed scientific literature.

Mr. [redacted] showed no statistically high FA values in 10 fiber tract regions. Fiber tract regions with high FA included the uncinate fasciculus which is known to be selectively vulnerable to traumatic forces. The fiber tract regions with high FA normally support a range of sensory, motor, and cognitive functions, including memory, attention, and executive function.

Overall, the volumetric and DTI data were statistically abnormal and consistent with a traumatic brain injury, but quantitative MRI and DTI analyses are not stand-alone tests for traumatic brain injury.

Quantitative imaging is part of a multifactorial evaluation of the possible neurobiological consequences of head trauma. Careful review of the quantitative imaging findings within the context of Mr. [redacted]'s developmental profile, medical history, timeline of symptom development, and additional radiological, neurological, neuropsychological, and/or psychiatric evaluations is needed to further clarify the etiology of these findings and their relationship to specific past events and her current status.

This report has been prepared by:

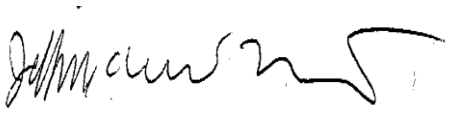

Jeffrey David Lewine, Ph.D.
Principal Neuroscientific Consultant, MINDSET
Affiliate Professor of Translational Neuroscience, The Mind Research Network
Director of Business Development, The Mind Research Network
Director of Neuroscience, Lovelace Scientific Resources
Adjunct Associate Professor of Neurology and Psychology, University of New Mexico

This Quantify Report provides an evaluation of the potential volumetric and diffusion tensor imaging consequences of neurobiological insults such as head trauma and toxic exposures. Additional information directly addressing the requirements of Federal Rules of Evidence 801/803 and 702 can be provided by directly contacting MINDSET at (505) 249-7058. Information in this report should only be interpreted by qualified experts with an understanding of the employed volumetric, DTI and statistical methods, plus knowledge of the underlying foundational research and peer-reviewed literature linking imaging finding to neurobiological status.

THE CONCUSSION GROUP

Edward L. Soll, M.D. Radiologist, Director
Jeffrey D. Lewine, PhD Translational NeuroScience

PATIENT
[redacted]
DOB: [redacted]
Gender: Male
Date of Exam: 02/24/2020
Date of Report: 03/05/2020

Review and Comment:

I have supervised the DTI DiCOM data acquisition process performed onsite at the MRN scanner partnered with The Concussion Group and reviewed the Mindset Volumetric/DTI analysis; and confirm that the MRI protocols as well as the applied analytic tools were methodically utilized as designed. I accept the final DTI and Volumetric Z-Scores as statistically appropriate.

Edward L. Soll, M.D.
Certified, American Board of Radiology 1973
Radiologist, Director, The Concussion Group

THE CONCUSSION GROUP

MINDSET (Quantify)

Figure 1: Mr. [redacted]
Z-scores for Regional Brain Volumes, Scaled by Total Intracranial Volume

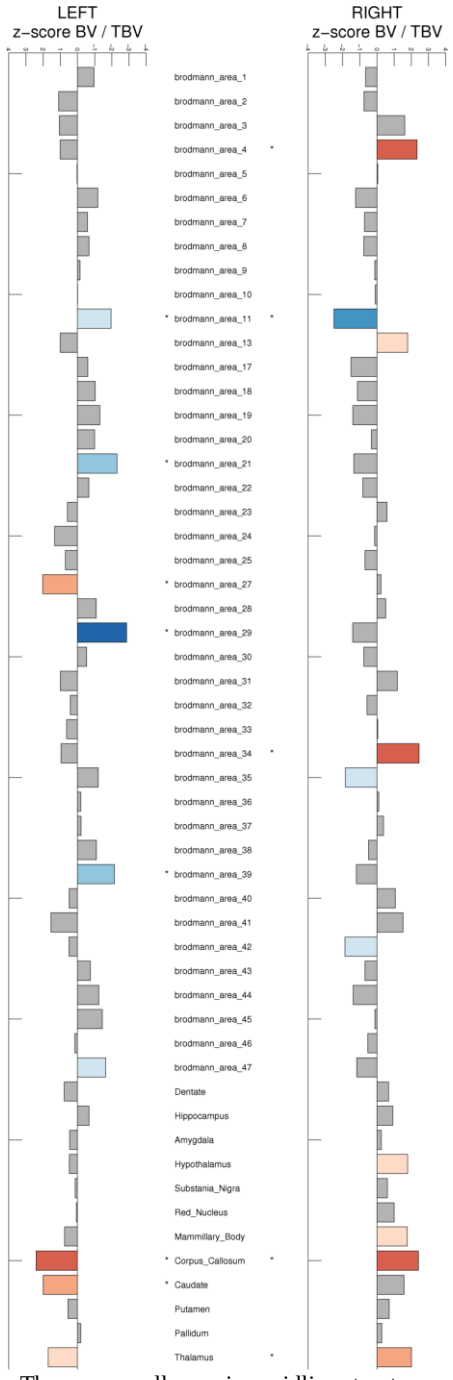

The corpus callosum is a midline structure.
Identical values are indicated in left and right columns.

Region-of-interest volumetric analyses

Data are shown as Z-score deviates based on comparison of client metrics with average metrics for a gender and age-range (+/- 10 years) matched group of **161** neuro-typical subjects.

At the level of individual isolated analyses:

Gray bars show brain regions with volumes that are within normal limits

Regions where the bar is red have abnormally high volume ($p<0.05$).

Regions where the bar is blue have abnormally low volumes ($p<0.05$).

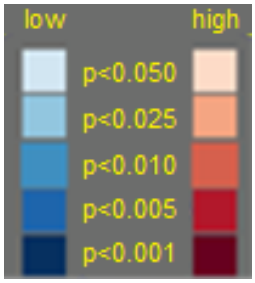

For Mr. [redacted], isolated evaluation of individual brain regions revealed 18 of 107 regions to show atypical volumes (8 low; 10 high).

However, only observations with an * survive correction for multiple comparisons.

Following correction for multiple comparisons, only 11 brain regions were still considered to show abnormal volumes from a statistical perspective (5 low; 6 high).

Low: Left: BA11, BA21, BA29, BA39
Right:BA11

High: Left: BA27, Caudate
Right:BA4, BA34, Thalamus Midline: Corpus Callosum

THE CONCUSSION GROUP

MINDSET (Quantify)

Figure 2: Mr. [redacted]
Brain Regions with Abnormal Volumes on Isolated Evaluation

Following correction for multiple comparisons**, only 11** of the brain regions with atypical volumes on isolated individual evaluation were still considered to be abnormal from a statistical perspective.

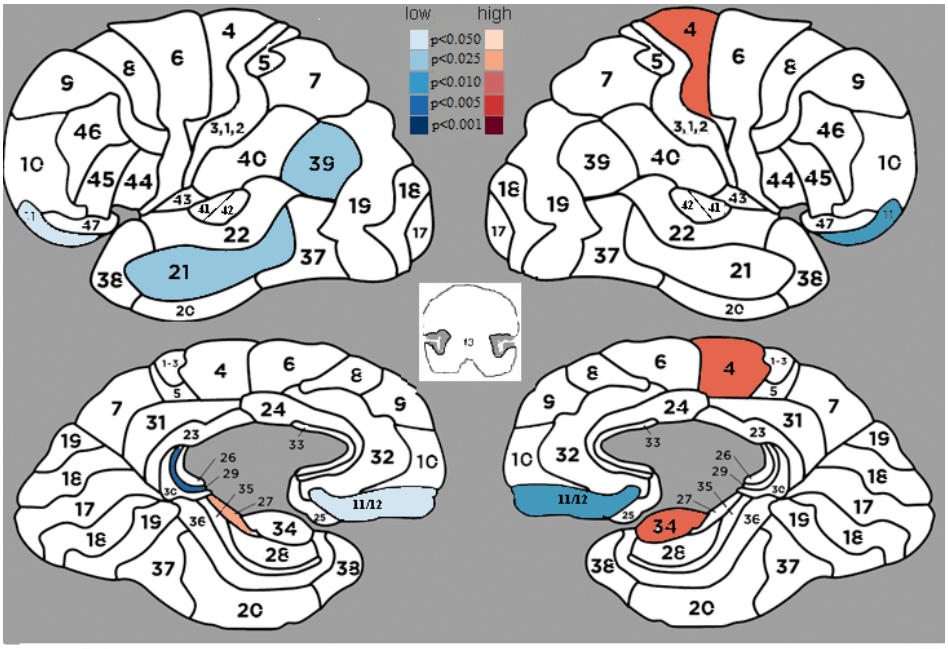

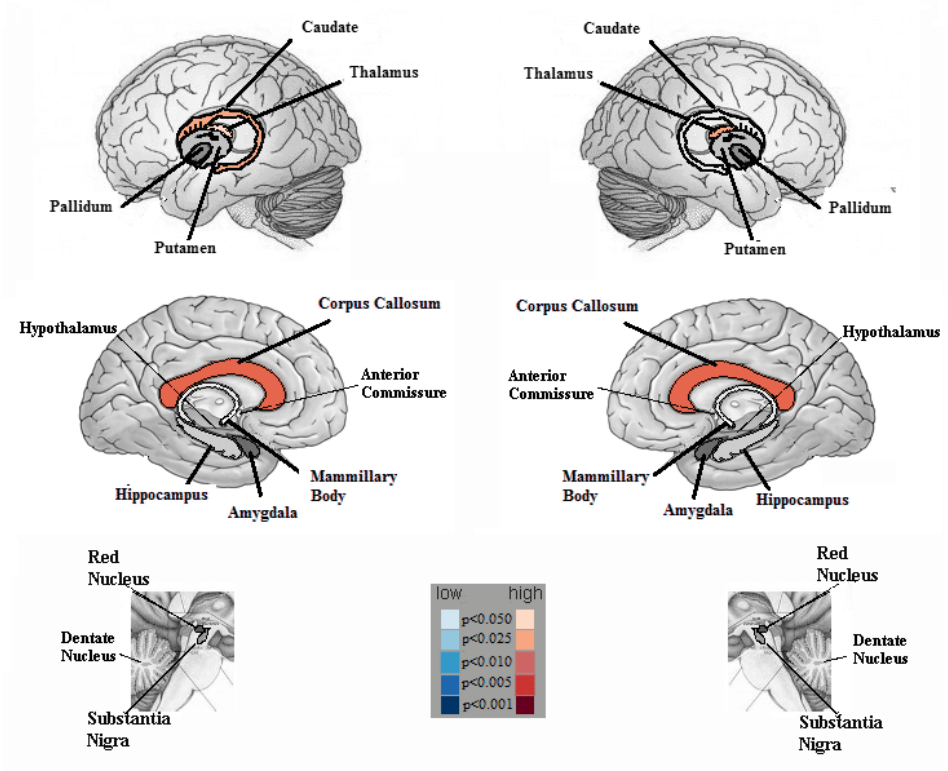

THE CONCUSSION GROUP

MINDSET (Quantify)

Table 1: Mr. [redacted]
Regions-of-Interest with Abnormal Volumes on Individual Evaluation

Following correction for multiple comparisons, **only 11** of the brain regions with atypical volumes on isolated individual evaluation were still considered to be abnormal from a statistical perspective.

Area		General Location	Supported Functions
Brodmann 1,2,3 combined	L/R	Primary somatosensory cortex	Tactile sensation
Brodmann 4	R*	Primary motor cortex	Motor control
Brodmann 5	L/R	Somatosensory association cortex	Tactile object recognition
Brodmann 6	L/R	Premotor and Supplementary motor cortex	Control of proximal and trunk muscles; Motor sequencing
Brodmann 7	L/R	Somatosensory association cortex	Visuo-spatial processing; Praxic abilities
Brodmann 8	L/R	Frontal eye fields	Planning of complex movements, control of eye movements
Brodmann 9	L/R	Dorsolateral Prefrontal Cortex	Executive Function, Working Memory
Brodmann 10	L/R	Anterior Prefrontal Cortex	Strategic Planning, Cognitive Branching
Brodmann 11	L*/R*	Orbital Frontal Cortex	Behavioral/Emotional Regulation, Behavioral Inhibition
Brodmann 13	R	Insula	Social emotions, multimodal sensory processing, salience
Brodmann 17	L/R	Primary Visual Cortex	Basic Vision
Brodmann 18	L/R	Secondary Visual Cortex	Shape recognition, visual attention
Brodmann 19	L/R	Association Visual Cortex	Visual-spatial processing, visual motion, face and word processing (L/R)
Brodmann 20	L/R	Inferior Temporal Gyrus	High-level visual information processing and recognition memory
Brodmann 21	L*	Middle Temporal Gyrus	Complex auditory processing and language
Brodmann 22	L/R	Superior Temporal Gyrus	Auditory processing, Receptive Language (Wernicke's area)
Brodmann 23	L/R	Posterior Cingulate Cortex	Emotion and Memory, Intrinsic Control
Brodmann 24	L/R	Anterior Cingulate Cortex	Behavioral Control, Reward Based Decision Making, Social Evaluation
Brodmann 25	L/R	Subgenual Ventromedial Prefrontal Cortex	Decision making, emotional processing, social behavior
Brodmann 27	L*	Periform Cortex	Olfaction
Brodmann 28	L/R	Ventral Entorhinal Cortex	Short-term memory
Brodmann 29	L*	Retrosplenial Cingulate Cortex	Episodic memory, navigation, imagination, and future planning
Brodmann 30	L/R	Part of Cingulate Cortex	Episodic memory, navigation, imagination and future planning
Brodmann 31	L/R	Dorsal Posterior Cingulate Cortex	Emotion and Memory, Intrinsic Control
Brodmann 32	L/R	Dorsal Anterior Cingulate Cortex	Behavioral Control, Reward Based Decision Making, Social Evaluation
Brodmann 33	L/R	Part of the Anterior Cingulate Cortex	Behavioral Control, Reward Based Decision Making, Social Evaluation
Brodmann 34	R*	Dorsal Entorhinal Cortex/Parahippocampal Gyrus	Olfaction, Short-term memory
Brodmann 35	R	Perirhinal Cortex	Memory, Emotion,
Brodmann 36	L/R	Ectorhinal Area	Short-term memory
Brodmann 37	L/R	Fusiform Gyrus	Word recognition (L) / Face Processing (R)
Brodmann 38	L/R	Temporopolar Regions	Memory, Language
Brodmann 39	L*	Angular Gyrus	Language, reading, mathematics, attention
Brodmann 40	L/R	Supramarginal Gyrus	Spatial perception, phonological choices
Brodmann 41	L/R	Primary Auditory Cortex	Basic Hearing
Brodmann 42	R	Auditory Cortex	Auditory processing
Brodmann 43	L/R	Gustatory Cortex	Taste
Brodmann 44	L/R	Pars opercularis, inferior frontal gyrus, part of Broca's area	Expressive Language
Brodmann 45	L/R	Pars triangularis, inferior frontal gyrus, part of Broca's area	Expressive Language
Brodmann 46	L/R	Dorsolateral Prefrontal Cortex	Executive Function, Working Memory
Brodmann 47	L	Pars orbitalis, inferior frontal gyrus	Syntax
Dentate Nucleus	L/R	Cerebellum	Planning and initiation of voluntary movements
Hippocampus	L/R	Medial Temporal Lobe	Short-term Memory
Amygdala	L/R	Medial Temporal Lobe	Emotion
Hypothalamus	R	Just left/right of Midline	Regulates autonomic functions, pituitary, hunger, sleep
Substantia Nigra	L/R	Brainstem	Dopaminergic motor control
Red Nucleus	L/R	Brainstem	Motor Coordination
Mammillary Body	R	Just left/right of Midline	Memory
Corpus Callosum	midline*	Midline	Interconnects L/R hemisphere
Caudate	L*	Part of the Basal Ganglia	Regulates movement, cognition
Putamen	L/R	Part of the Basal Ganglia	Regulates movement
Pallidum	L/R	Part of the Basal Ganglia	Regulates movement
Thalamus	L/R*	Just left/right of Midline	Sensory, Motor, Emotional and Cognitive Functioning

Low volumes may reflect perturbation of early developmental processes, malnutrition, toxic stress, toxic exposures, or more commonly neurological/psychiatric disease and/or brain injury.

High volumes may reflect perturbation of early developmental pruning, enhanced skill development, brain injury related edema, astrogliosis, and/or compensatory reactions to damage in other areas.

THE CONCUSSION GROUP

MINDSET (Quantify)

Figure 3: Mr. [redacted] Z-scores for FA Values

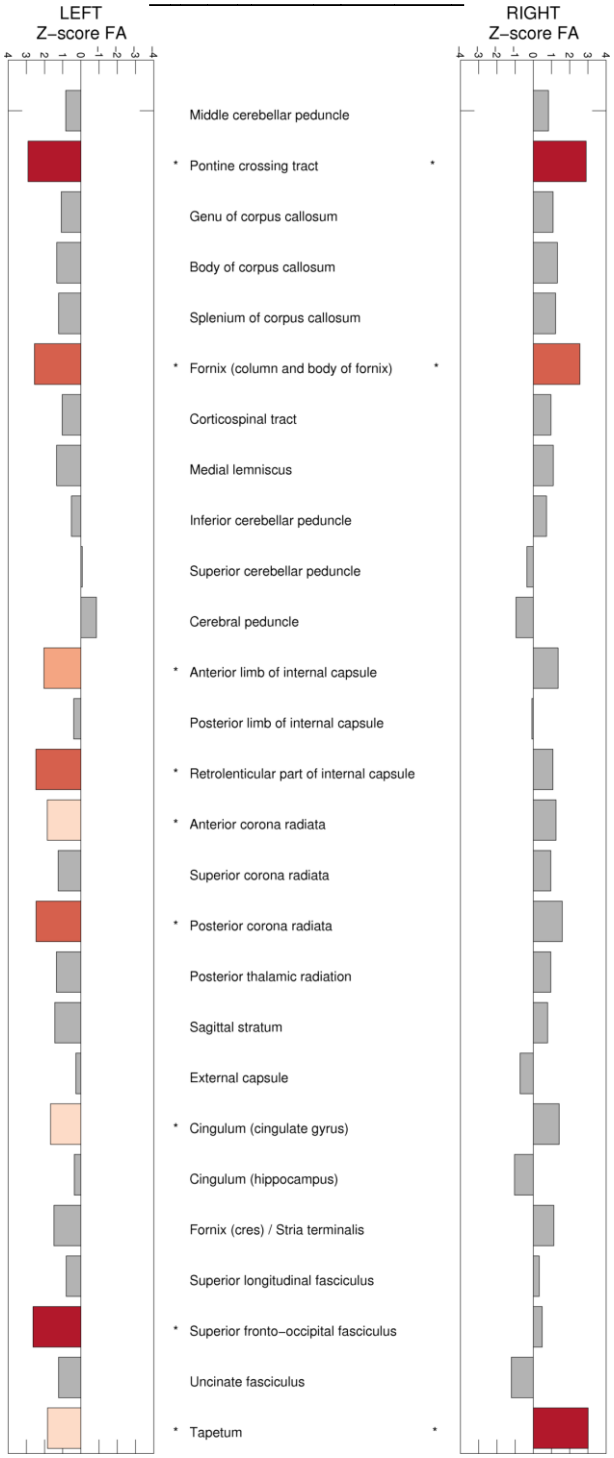

The first 6 tracts are at the midline and without separable left/right components. Identical values are plotted in left and right columns.

FA Values for Fiber Tract Regions

Data are shown as Z-score deviates based on comparison of client metrics with average metrics for a gender and age-range (+/- 10 years) matched group of **161** neuro-typical subjects.

At the level of individual isolated analyses:

Gray bars show fiber tract regions with FA values that are within normal limits
Tracts where the bar is red have abnormally high FA values ($p<0.05$).
Tracts where the bar is blue have abnormally low FA values ($p<0.05$).

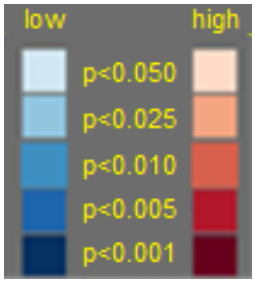

For Mr. [redacted], isolated evaluation of individual fiber tract regions revealed 10 of 48 regions to show atypical FA values (0 low; 10 high).

However, only observations with an * survive correction for multiple comparisons.

Following correction for multiple comparisons, All 10 fiber tract regions were still considered to show abnormal FA values from a statistical perspective (0 low; 10 high).

THE CONCUSSION GROUP

MINDSET (ΩμΛNτίfγ)

Table 2 – Mr. [redacted]
FA Values on Individual Isolated Evaluation

Following correction for multiple comparisons**, ALL 10** fiber tract regions with atypical FA values on isolated individual evaluation were still considered to be abnormal from a statistical perspective.

#	Regions	Client	Database	Stdev	Z-score
1	Middle cerebellar peduncle	0.463	0.449	0.017	0.839
2*	Pontine crossing tract (a part of MCP)	0.518	0.433	0.029	2.902
3	Genu of corpus callosum	0.667	0.645	0.020	1.086
4	Body of corpus callosum	0.719	0.681	0.029	1.327
5	Splenium of corpus callosum	0.774	0.752	0.018	1.226
6*	Fornix (column and body of fornix)	0.516	0.393	0.048	2.558
7	Corticospinal tract R	0.461	0.433	0.029	0.967
8	Corticospinal tract L	0.480	0.446	0.033	1.030
9	Medial lemniscus R	0.578	0.549	0.026	1.100
10	Medial lemniscus L	0.589	0.555	0.026	1.339
11	Inferior cerebellar peduncle R	0.431	0.412	0.027	0.722
12	Inferior cerebellar peduncle L	0.429	0.413	0.030	0.520
13	Superior cerebellar peduncle R	0.540	0.548	0.023	-0.352
14	Superior cerebellar peduncle L	0.524	0.526	0.022	-0.076
15	Cerebral peduncle R	0.623	0.643	0.021	-0.954
16	Cerebral peduncle L	0.641	0.658	0.020	-0.850
17	Anterior limb of internal capsule R	0.560	0.534	0.019	1.361
18*	Anterior limb of internal capsule L	0.573	0.535	0.019	2.035
19	Posterior limb of internal capsule R	0.591	0.593	0.018	-0.080
20	Posterior limb of internal capsule L	0.616	0.609	0.018	0.392
21	Retrolenticular part of internal capsule R	0.579	0.553	0.024	1.074
22*	Retrolenticular part of internal capsule L	0.648	0.590	0.024	2.472
23	Anterior corona radiata R	0.464	0.434	0.024	1.249
24*	Anterior corona radiata L	0.465	0.423	0.023	1.845
25	Superior corona radiata R	0.472	0.454	0.019	0.964
26	Superior corona radiata L	0.499	0.474	0.020	1.255
27	Posterior corona radiata R	0.478	0.441	0.023	1.592
28*	Posterior corona radiata L	0.496	0.439	0.023	2.463
29	Posterior thalamic radiation R	0.573	0.548	0.026	0.962
30	Posterior thalamic radiation L	0.569	0.535	0.025	1.344
31	Sagittal stratum R	0.515	0.498	0.022	0.788
32	Sagittal stratum L	0.513	0.481	0.022	1.435
33	External capsule R	0.380	0.395	0.021	-0.725
34	External capsule L	0.437	0.431	0.024	0.278
35	Cingulum (cingulate gyrus) R	0.498	0.460	0.027	1.428
36*	Cingulum (cingulate gyrus) L	0.551	0.505	0.028	1.672
37	Cingulum (hippocampus) R	0.340	0.370	0.029	-1.030
38	Cingulum (hippocampus) L	0.390	0.378	0.034	0.370
39	Fornix (cres) / Stria terminalis R	0.477	0.450	0.024	1.128
40	Fornix (cres) / Stria terminalis L	0.546	0.504	0.028	1.482
41	Superior longitudinal fasciculus R	0.445	0.438	0.023	0.322
42	Superior longitudinal fasciculus L	0.478	0.459	0.023	0.811
43	Superior fronto-occipital fasciculus R	0.475	0.461	0.028	0.488
44*	Superior fronto-occipital fasciculus L	0.531	0.448	0.032	2.630
45	Uncinate fasciculus R	0.391	0.432	0.034	-1.208
46	Uncinate fasciculus L	0.473	0.432	0.034	1.231
47*	Tapetum R	0.465	0.372	0.031	3.015
48*	Tapetum L	0.362	0.305	0.031	1.837

Client FA value abnormally high, p<0.05 (isolated, individual testing)
Client FA value abnormally low, p<0.05 (isolated, individual testing)
* indicates survival of correction for multiple comparisons

THE CONCUSSION GROUP

MINDSET (ΩμANτifγ)

Table 3: Mr. [redacted]
Fiber Tract Regions of Interest with Abnormal FA Values on Individual Isolated Evaluation

Following correction for multiple comparisons, **ALL 10** fiber tract regions with atypical FA values on isolated individual evaluation were still considered to be abnormal from a statistical perspective.

.

JHU White Matter Atlas Fiber Tract Regions		Connections	Supported Functions
Middle Cerebral Peduncle	Midline	Interconnects Cerebellum and Pons	Initiation and Timing of Volitional Movement
Pontine Crossing Tracts	Midline*	Interconnects Pons and Contralateral Cerebellum	Coordination of Movement
Genu of the Corpus Callosum	Midline	Interconnects Right and Left Anterior Frontal Lobes	Interhemispheric Integration of Executive Functions
Body of the Corpus Callosum	Midline	Interconnects Right and Left Posterior Frontal Lobes Interconnects Right and Left Parietal Lobes	Interhemispheric integration of Motor and Somatosensory Functions
Splenium of the Corpus Callosum	Midline	Interconnects Right and Left Occipital Lobes	Interhemispheric Integration of Visual Functions
Fornix	Midline*	Interconnects the Hippocampus and Mammillary Bodies	Short-Term Memory
Corticospinal Tracts	L/R	Connects Primary Motor Cortex with Contralateral Spinal Motor Neurons	Motor Control of the Contralateral Side of the Body
Medial Lemniscus	L/R	Connects Dorsal Column Nuclei with the Contralateral Thalamus (VPL)	Somatosensory Perception of the Contralateral Side of the Body
Inferior Cerebellar Peduncles	L/R	Connects Spinal Cord and the Medulla to the Cerebellum	Posture, Balance, and Coordination
Superior Cerebellar Peduncles	L/R	Interconnects Cerebellum to Pons and Midbrain	Motor Coordination and Balance
Cerebral Peduncles	L/R	Interconnects Cerebellum with the Thalamus and Motor Cortex	Motor Control
Anterior Limb of the Internal Capsule	L*	Contains Fibers Interconnecting the Thalamus and Frontal Lobe; Lentiform and Caudate Nuclei; Cortex and Corpus Striatum	Motor Control; Higher Cognitive Function
Posterior Limb of the Internal Capsule	L/R	Contains Fibers Interconnecting Motor Areas with the Brainstem; Midbrain and the Thalamus, Occipital Lobes, and Temporal Lobes	Visual-Spatial Processing, Visual Motion, Face and Word Processing (L/R)
Retrolenticular Part of the Internal Capsule	L*	Interconnects Thalamus and Occipital Cortex	Visual Processing
Anterior Corona Radiata	L*	Contains Descending and Ascending Fibers Related to Cortex – especially for the Frontal Lobes	Executive Function, Emotional Control
Superior Corona Radiata	L/R	Contains Descending and Ascending Fibers Related to Cortex – especially for the Motor Cortex	Motor Control
Posterior Corona Radiata	L*	Contains Descending and Ascending Fibers Related to Cortex – especially for the Parietal Lobes	Attentional Control, Somatosensory Function
Posterior Thalamic Radiation	L/R	Interconnects Thalamus and Cortex	Visual and Auditory Function
Sagittal Stratum	L/R	Interconnects Thalamus with Occipital, Parietal, Temporal and Cingulate Cortices	Visual, Auditory, and Cognitive Function
External Capsule	L/R	Contains Cortico-Cortical Association Fibers for Occipital, Temporal, Parietal, and Cingulate Cortices	Cognitive Processing
Cingulum (cingulate cortex)	L*	Interconnects Cingulate and Pre-Frontal Cortices	Cognitive Processing and Decision Making
Cingulum (hippocampus)	L/R	Interconnects Cingulate and Entorhinal Cortices	Memory, Emotional Processing
Fornix (cres) and Stria Terminalis	L/R	Interconnects Hippocampus and Mammillary Bodies; Amygdala with the Septal Region and Hypothalamus	Memory, Emotional Processing, Fear Response
Superior Longitudinal Fasciculus	L/R	Interconnects the Front and Back of the Cerebrum, Including Frontal, Parietal, Occipital, and Cingulate Areas	Higher Cortical Functions including Language, Attention, Motor Control, and Spatial Processing.
Superior Fronto-Occipital Fasciculus	L*	Interconnects the Frontal Lobe with the Occipital and Parietal Lobes	Spatial Awareness
Uncinate Fasciculus	L/R	Interconnects Hippocampus and Amygdala with Orbital Frontal Cortex	Memory, Emotional Processing, Language
Tapetum	L*/R*	Contains Commissural Fibers Interconnecting Right and Left Temporal Lobes	Interhemispheric Integration for Auditory Processing

Client FA value abnormally high, p<0.05 (isolated, individual testing)
Client FA value abnormally low, p<0.05 (isolated, individual testing)
* indicates survival of correction for multiple comparisons

Standard Associated MRI Brain Report

TO: DR. [redacted]
[redacted]
[redacted]

FAX: [redacted]

NAME: [redacted]
MRN# [redacted]
DOB: [redacted]
GENDER: Male
DATE OF SERVICE: 02/24/2020
REFERRING PHYS: DR. [redacted]

EXAM: MRI BRAIN WITHOUT CONTRAST

HISTORY: POSTCONCUSSIONAL SYNDROME; DATE OF INJURY - 02/06/2018. MVC with headache, slurred speech, memory problems confusion.

COMPARISON: None

TECHNIQUE: Multiplanar multisequence MR imaging of the brain was obtained on a Siemens 3 Tesla magnet without gadolinium.

A DTI acquisition was obtained in addition to the standard technique protocol and after analysis, a separate quantitative DTI report along with a volumetric analysis will be subsequently rendered.

FINDINGS:

There is no restricted diffusion.

No significant gliotic white matter signal changes are present.

The pituitary gland, midbrain, cerebellum, and upper cervical cord are normal in signal and morphology.

There is no pathologic fluid collection. The ventricular system and basilar cisterns are appropriate in size and configuration. Normal flow voids are noted in the major cerebral blood vessels.

Orbits, orbital contents, middle ears and mastoids appear unremarkable.

The visualized paranasal sinuses are clear.

CONCLUSION:

Negative MRI of the brain without gadolinium.

INTERPRETING RADIOLOGIST: [redacted], MD
THIS DOCUMENT HAS BEEN ELECTRONICALLY SIGNED 02/26/2020 at 3:46 PM (CST)
ACCESSION #: [redacted]

THE CONCUSSION GROUP

MINDSET (Ωμ^ANτifγ)

MRI-APPENDIX-I

Basic Concepts in Brain Organization, Magnetic Resonance Imaging, and Quantitative Assessment of Regional Brain Volumes and Diffusion Tensor Parameters

THE CONCUSSION GROUP

MINDSET (Quantify)

BASIC CONCEPTS IN BRAIN ORGANIZATION, MAGNETIC RESONANCE IMAGING AND TRAUMATIC BRAIN INJURY

Brain Organization:

The human brain is composed of more than 100 billion cells, including neurons and supporting glial cells. Electrochemical signals are used to encode and transmit information within brain cells, with neurotransmitters used to transfer information from one neuron to another across synapses. Neurons have three key parts: (1) the dendrites, which bring information into the cell, (2) the cell body, which integrates the information, and (3) the axon, which takes information to the next cell. As illustrated in figure 1, within the brain, cell bodies often cluster together to give what is known as gray matter. Axons often travel together in tracts, in what is known as the white matter, where they connect different parts of the brain. The outermost gray matter region of the brain is known as the cerebral cortex. Cells may be arranged differently in different parts of the cortex. This, along with the specific local and distant interconnections between cells gives rise to cortical specialization and networks – that is, the brain is partly organized into functional modules and networks supporting different calculations and behavioral abilities (see figure 2).

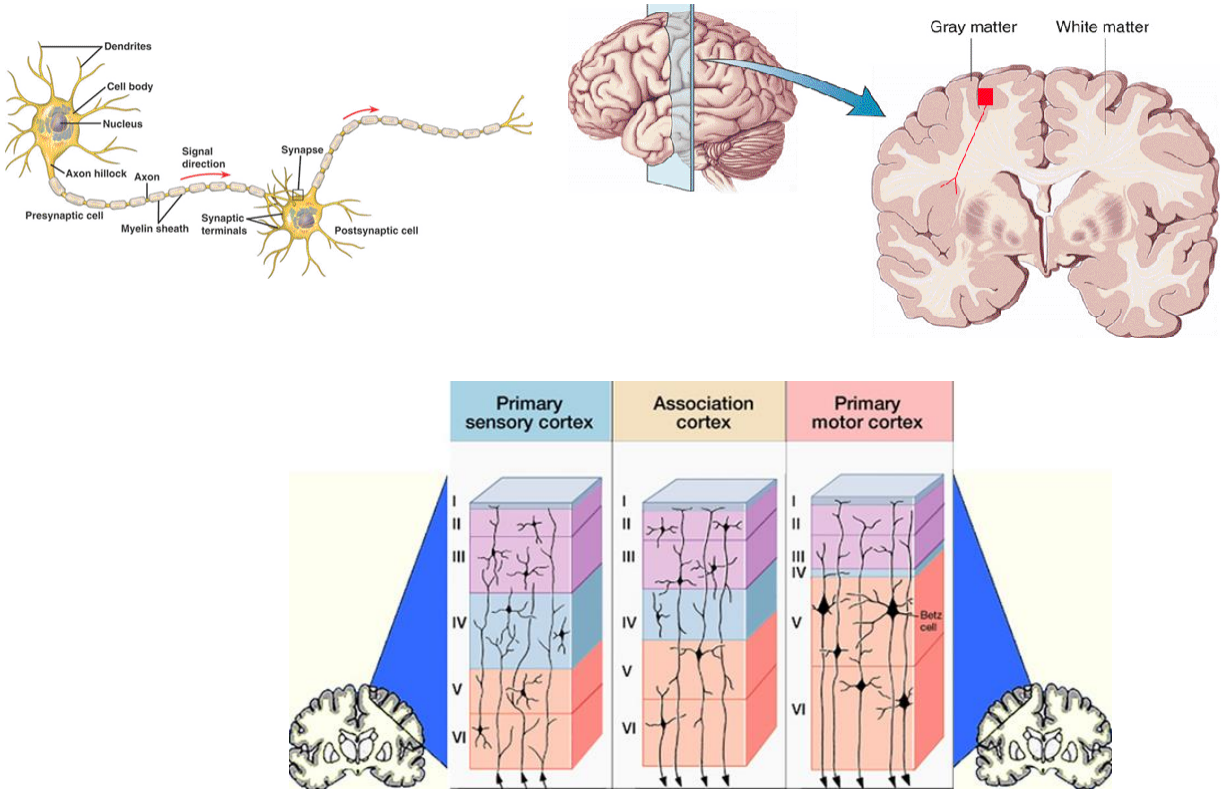

Figure 1: Neurons and Brain Organization: Neurons are composed in a cell body, with radiating dendrites that bring information into the cell, and an axon which carries information to the next cell. The axon of one cell forms synapses with dendrites of other cells. Cell bodies and dendrites cluster around the periphery of the brain in the gray matter of the cerebral cortex, and also in nuclei near the center of the brain. The axonal fibers which interconnect one brain region to another may travel in fiber bundles that are part of white matter. Cells are arranged in different ways in different brain regions. This, together with the specific connections of each region supports specialized functions.

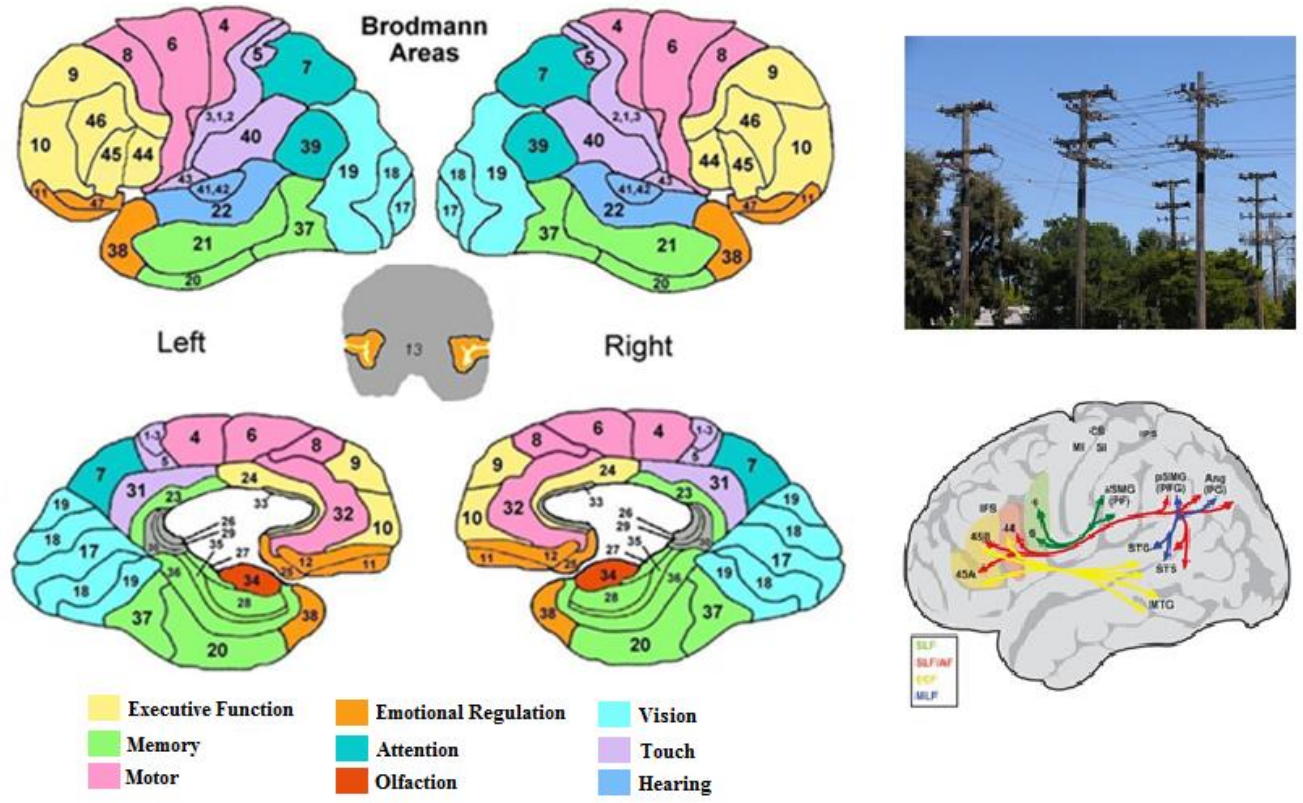

Figure 2: Different areas of the brain are specialized for different behavioral processes. Also, the processing modules are interconnected by white matter fibers (much like telephone cables) to form functional networks that can support complex abilities like language, decision making, emotional regulation, impulse control, and mnemonic processing. Structural or functional damage to either the modules or their interconnections can have devastating behavioral consequence.

Magnetic Resonance Imaging

Magnetic Resonance Imaging (MRI) is a non-invasive technique for evaluating structure and function. Briefly, by examining how the hydrogen protons of water molecules behave when placed within a steady magnetic field and bombarded by pulses of radio-wave energy, the MRI system can reconstruct a picture of the brain's anatomy. By altering the parameters and sequence of radio-wave pulses, it is also possible to explore the white matter interconnections between brain regions, brain biochemistry, metabolism, and hemodynamics (see figure 3).

Imaging evaluations in patients with brain injury often include T1-weighted, T2-weighted, FLAIR, SWI and DTI sequences. T1-weighted imaging provides exceptional gray-white matter differentiation and a detailed picture of brain anatomy. T2 and FLAIR imaging are especially useful for identifying edema and lesions in the white matter. SWI – susceptibility weighted imaging – is very sensitive to iron deposition associated with bleeding caused by stroke or small hemorrhages caused by traumatic brain injury. DTI – Diffusion Tensor Imaging examines the diffusion properties of water within the brain and thereby provides insight into the integrity of axonal tracts (which normally restrict the direction of water diffusion to be along [rather than across] the direction of the tracts).

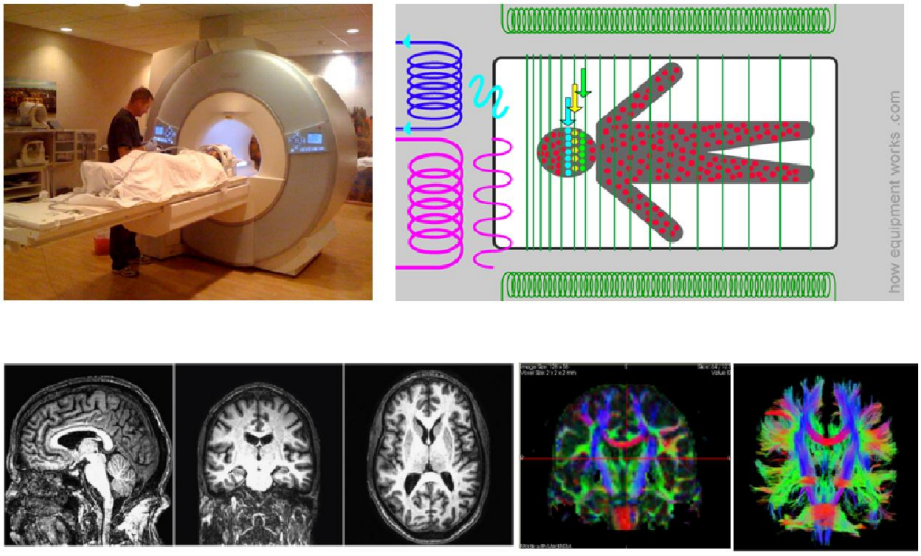

Figure 3: Basic concepts in MRI. The subject is placed within a strong steady magnetic field and radiofrequency pulses are used to excite the hydrogen protons of water molecules in the brain. By examining how the protons behave, images of brain structure and function can be generated. The images on the lower left are obtained using a T1-weighted pulse sequence which is ideal for exploring the anatomical detail of the brain. The color images in the lower right show the results of Diffusion Tensor Imaging and associated tractography, MR-based methods for exploring the integrity of connections between brain regions.

Clinical, visual inspection of MR data can often reveal major pathologies like tumors, multiple sclerosis, and severe head trauma (see figure 4, for examples).

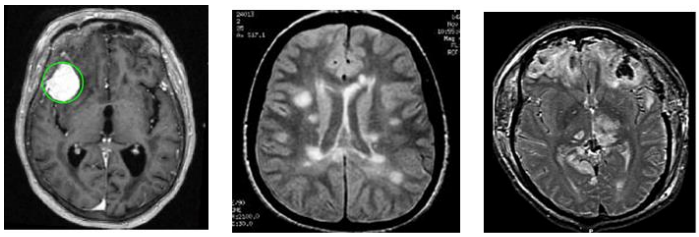

Figure 4: Example MRI findings in major pathological conditions

However, more mild injuries, such as those associated with a concussion, only rarely produce MR changes that can be seen on routine visual inspection. For example, less than 20% of subjects who suffer mild head trauma or a concussion will be reported to have abnormalities on a routine clinical MRI or CT. In cases like these, sophisticated quantitative data analytic procedures are needed to reveal injury. Of particular utility are (1) quantitative analyses of regional brain volume (that is, measurement of the size of various brain regions as visualized on T1-weighted images), and (2) a quantitative assessment of the integrity of white matter pathways (as indexed by Fractional Anisotropy (FA) on DTI), although even with these sophisticated approaches, >30% of mild TBI patients still have evaluations within normal limits.

Volumetric Analyses

Based on visual inspection alone, it is often difficult to determine if the size of a particular brain region (e.g., the hippocampus) is smaller than expected as a result of on an injury. Indeed, it is not uncommon for experts to

disagree on visual appearance. To avoid this problem and move analyses and interpretation from subjective opinion to objective scientific fact, automated computational methods can be employed. These methods provide quantitative measures of the actual volume of brain structures for each client, and they allow for a statistical comparison of the client's data with respect to data from a large group of neuro-typical subjects.

The brain is a 3-Dimensional structure that can be divided into small cubes, known as voxels, as shown in figure 5. For MRI images, an automated computer algorithm can, in each voxel, measure the amounts of gray matter, white matter, and cerebrospinal fluid (CSF). The computer can also divide the brain into regions-of-interest, based on known structural-functional relationships. For example, the computer can determine which voxels comprise brain regions like the hippocampus or primary motor cortex and thereby calculate the total amount of brain tissue in these regions for each individual client.

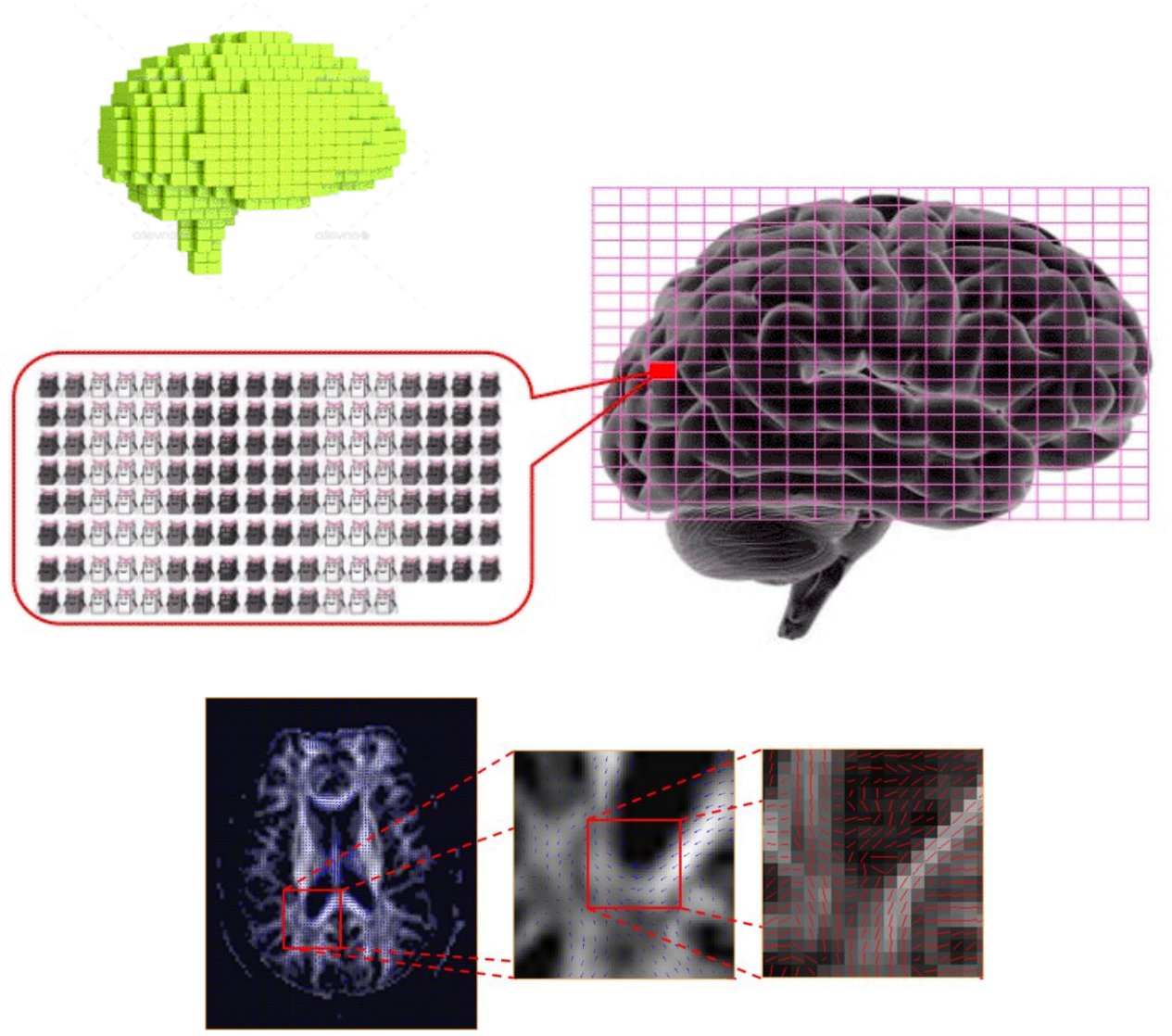

Figure 5: The brain as imaged using MRI can be divided into small voxels. In each voxel we can measure the density and volume of gray versus white matter.

Briefly, for volumetric analyses, MINDSET uses SPM12 correct for bias-field inhomogeneities, transform the data into MNI space, segment the data, and extract volume-related metrics. For region of interest volumetric analyses, MATLAB scripts are then used to divide the brain into 107 cortical and subcortical areas derived from TD-Brodmann (Lancaster, 2000) and AAL atlases (Tzourio-Mazoyer, et al., 2002). Figure 6 shows cortical regions from the TD-Brodmann atlas. Additional areas of interest include the basal ganglia and other subcortical motor nuclei, the thalamus, hippocampus, amygdala, and corpus callosum. To correct for variability in head/brain size, values are scaled by total intracranial volume or total brain volume prior to statistical evaluation.

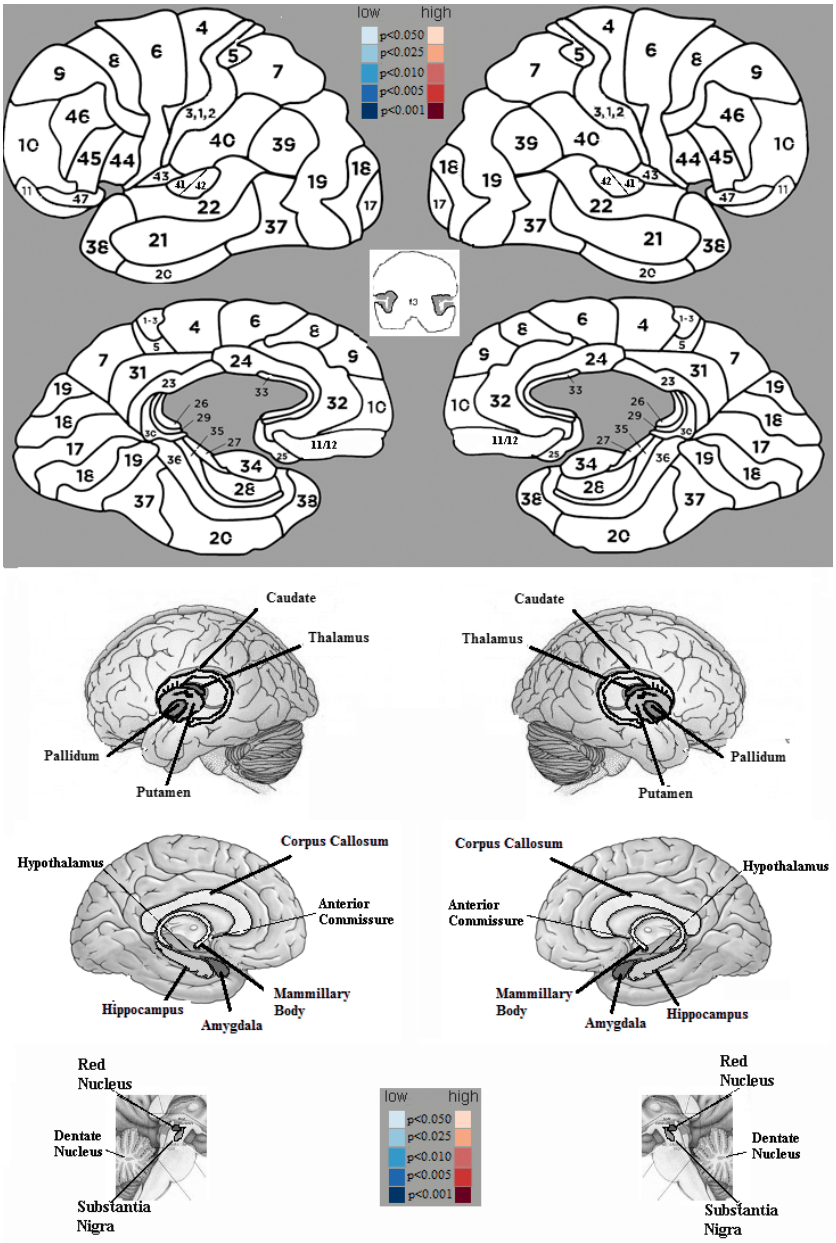

Figure 6: Pre-Selected TD-Brodmann and AAL Cortical and Sub-Cortical Regions of Interest

To determine if client metrics statistically deviate from within normal limits, MINDSET employs a normative database with volumetric and DTI data from >1000 neurotypical subjects. All normative MRI datasets had been collected previously using a 12-channel head-coil and a Siemens 3.0 Tesla TIM-TRIO MRI system located at the Mind Research Network (MRN) in Albuquerque, New Mexico. The database was created by pooling datasets across control groups for 36 IRB-approved studies. For membership in the neuro-typical control group of each study, a reported history of traumatic brain injury, or report of a diagnosed neurological or psychiatric disease or injury, substance use disorder, learning disability, or developmental disability was exclusionary.

The Concussuion Group (TCG) and MRN scanners are of the same type (3.0 T). TCG data acquisition parameters are identical to those which were used by MRN in the collection of the control datasets. The data analysis software algorithms, procedures, and processing pipeline used to assess data from TCG clients and the MRN control subjects were identical. Nevertheless, even when identical procedures are employed on a common type of MRI scanner, there is some inter-site variability in extracted metrics. Therefore, prior to statistical analyses, data metrics from TCG scanner are harmonized to those of the MRN scanner using a human physical phantom scaling procedure (see Palicios et al., 2017; Venkatraman et al., 2015). Briefly, two human subjects were scanned on both TCG and MRN machines and a set of region-specific scaling factors was then calculated to match the data from the TCG acquisition to the data from the MRN acquisition. These factors provide for harmonization of TCG and MRN datasets and allow TCG Image data to be validly evaluated with respect to the MINDSET/MRN normative database.
MATLAB scripts are then used to perform statistical analyses. Statistical evaluation of client data is based upon comparison of client metrics with sex and age-range matched control subjects drawn from the MINDSET database, typically with an age range of +/- 10 years. Standard univariate procedures are used to generate Z-scores for each individual metric.

To account for multiple comparisons, a Benjamini-Hochberg procedure with a false discovery rate of 25% is additionally applied. All procedures are performed in a completely automated and objective manner, free of any bias or client information other than gender and age.

Figure 7 shows the processing pipeline, with Figures 8 and 9 giving example output graphics.

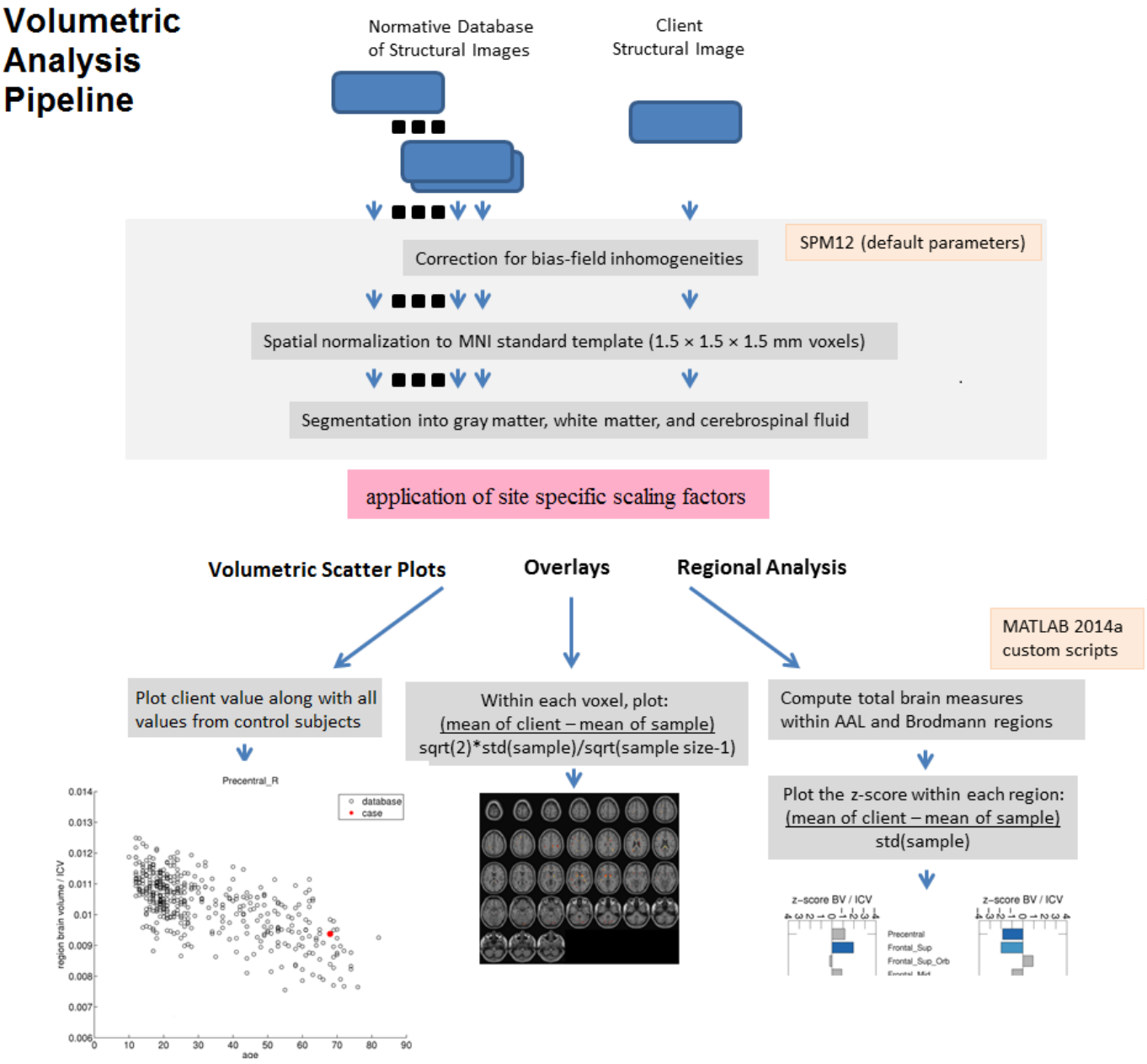

Figure 7: Volumetric Processing Pipeline

Neurotypical Control Subject

Head Trauma Client

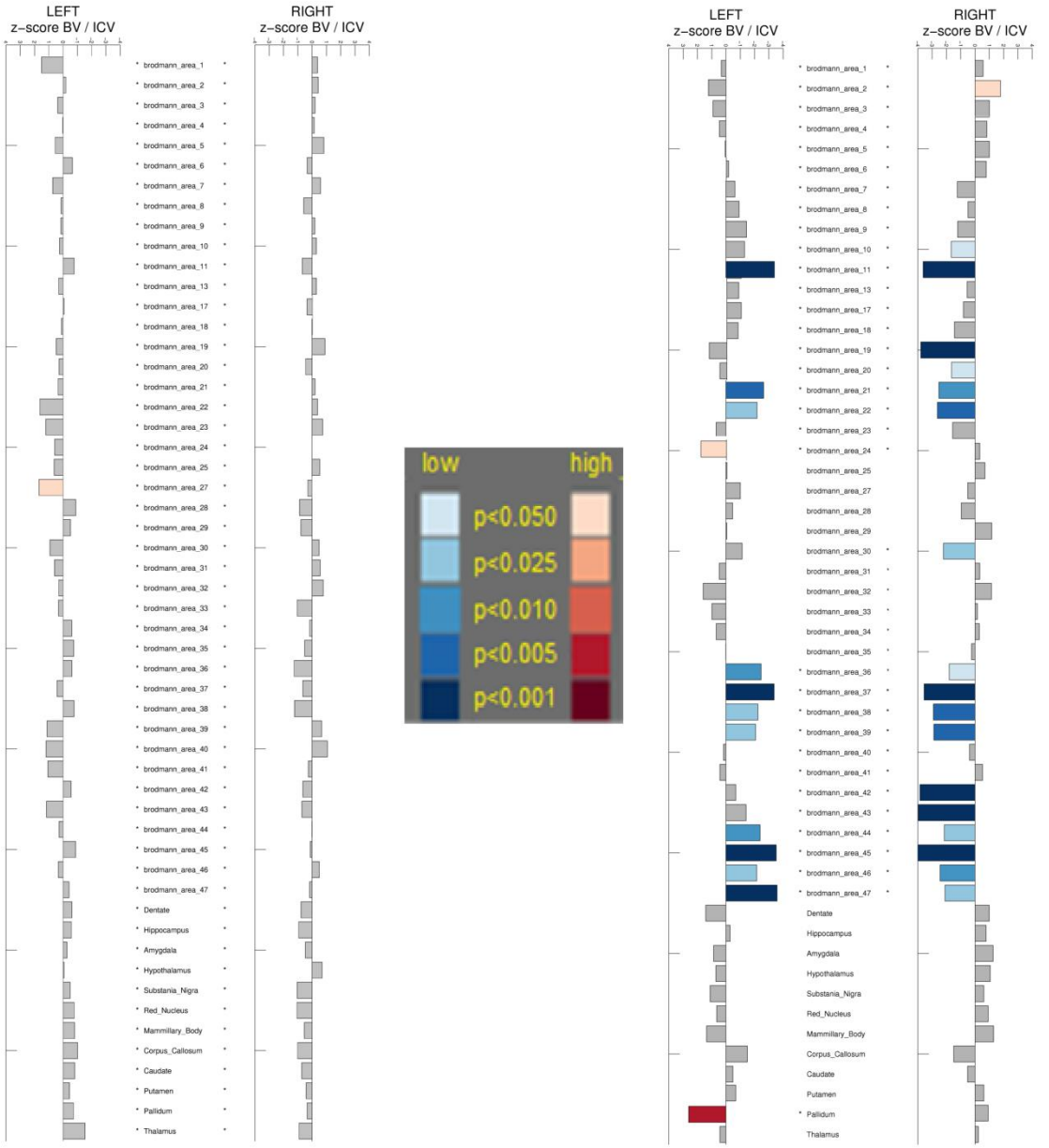

Figure 8:** Main Bar Plot Outputs. Bar plots show z-score deviations from the normative database, in the indicated region. Examples are shown for a neurotypical control subject and a head trauma client. Gray indicates regions that are not statistical significant (-1.645 < z < 1.645; p>0.05). Red indicates that a region has an atypically large volume (z > 1.645; p<0.05). Blue indicates that a region has an atypically low volume (z < -1.645, p<0.05). To correct for multiple comparisons, a Benjamini-Hochberg procedure is used with a False Discovery Rate of 25%. A region is ultimately considered to show a statistically significant deviation from normal if, and only if, it is abnormal on individual, isolated evaluation(p<0.05) <u>and</u> it survives correction for multiple comparisons. Such regions are designated by an *. For the example control subject, left Brodmann area 27 has a z-score of ~ 1.71, which is above of p<0.05 threshold of z = 1.645, so the bar is colored red. However, this observation does not survive correction for multiple comparisons, so it is not ultimately considered to be significant (so no * is provided). In contrast, the example head trauma client has 27 regions of significantly low volumes (blue bars with z-scores < -1.64) and a three regions with abnormally high regional volumes. All of the client regions that are significant on individual isolated evaluation survive correction for multiple comparisons. That is, each of these 30 regions (27 low; 3 high) is ultimately considered to show statistically significant deviation from normal (as indicated by the *).

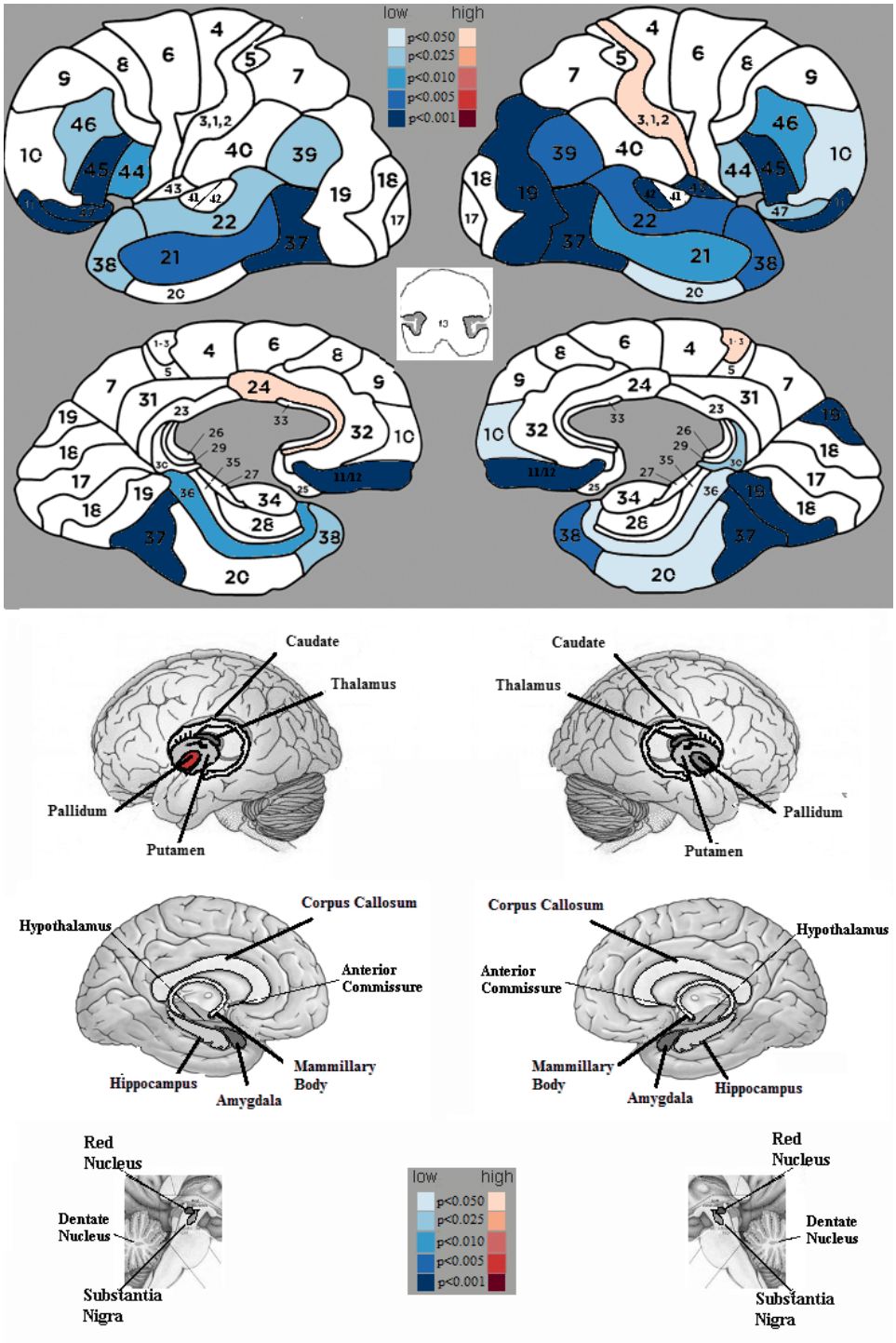

white/gray – volume within normal limits
red – high volume
blue – low volume

Figure 9: Anatomical map showing regions of abnormal volume for the Head Trauma Client shown in figure 8.

Diffusion Tensor Imaging (DTI)

Diffusion tensor imaging provides insight into the integrity of white matter tracts by measuring the diffusion properties of water within the brain. Imagine, for example, that you put a drop of ink in the middle of the ocean. The ink would spread (diffuse) in all directions equally. This is called isotropic diffusion (see figure 10). Now imagine that the ocean was filled with a bunch of pipes running in a common direction. In this case, the ink would spread in a preferred direction along the pipes, since it cannot easily penetrate into/across the pipes. When the ink diffuses in a preferential direction, this is called anisotropic diffusion. The brain is like the ocean filled with pipes – axons running within oriented fiber tracts. So, within the brain, water diffuses in preferred directions based on the local white matter anatomy. Using Diffusion Tensor Imaging the preferred direction of water movement within each voxel can be characterized by Fractional Anisotropy (FA), a value from 0 to 1, where 0 indicates isotropic diffusion and 1 indicates fully restricted diffusion in a single direction.

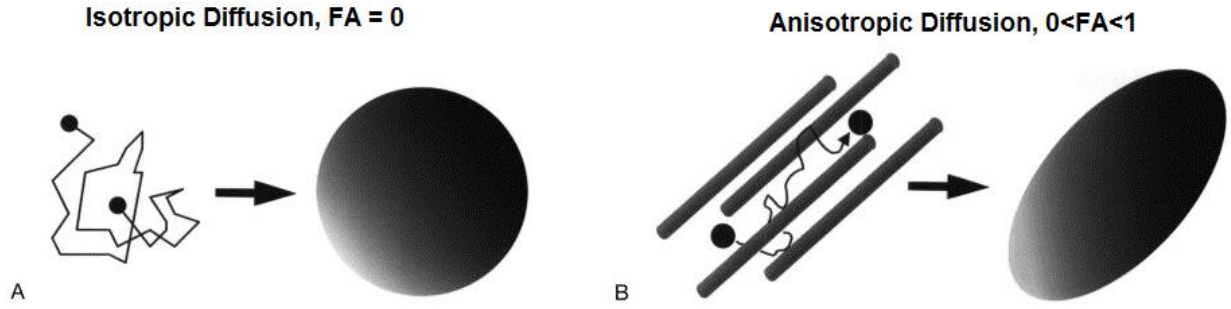

Figure 10: Basic Principles of DTI.

Typical diffusion tensor images color code the preferred directions of tracts, with color intensity indicating FA values, as shown previously in the lower right hand panels of figure 3. A process known as tractography can be used to reconstruct tract trajectories based upon FA values.

Just as was described for region-of-interest analyses in volumetric assessments, a computer algorithm can identify white matter tracts within the brain of each client and determine the average FA value for each tract. This client-specific value can then be statistically assessed with respect to a normative dataset. Abnormally low FA values are indicative of a breakdown in the normal organization of white matter tracts, as may be caused by traumatic injuries leading to myelin breakdown, and/or shrinkage or loss of axonal fibers. Abnormally high FA values can be associated with increased structural connectivity (as sometimes seen in epileptogenic networks or certain developmental disorders), intracellular axonal swelling (which causes compression of the extracellular space), acute inflammation with microglial activation, and/or reactive astrogliosis and compaction of neurofilament.

For DTI, the FLIRT algorithm in combination with the DTIFIT tool in FSL was used to compute FA maps with SPM alignment to the MNI FA template and subsequent extraction of tract-based FA values within the 48 fiber tracts defined by the Johns Hopkins University MRI Atlas of Human White Matter (Mori et al., 2009). Figure 11 shows the processing pipeline. Subsequent figures information on the 48 tract regions in the JHU atlas.

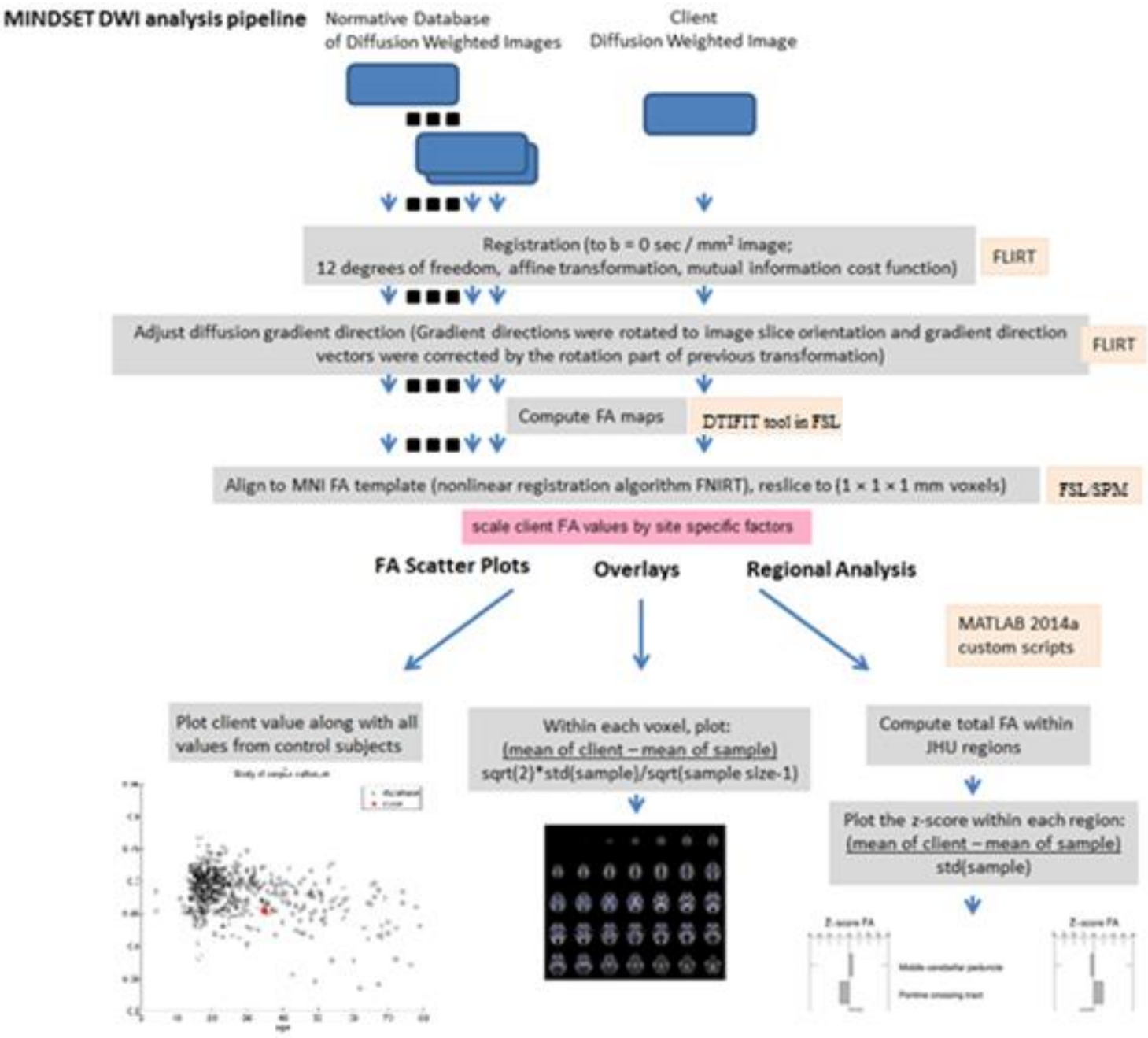

Figure 11: DTI data processing pipeline.

THE CONCUSSION GROUP

MINDSET (Quantify)

Johns Hopkins University White Matter Atlas Fiber Tract Regions

(images from Connectopedia Knowledge Database: www.fmritools.com/kbd)

Tract 1: Middle Cerebellar Peduncle
Connects: Cerebellum and Pons
Function: Initiation and timing of volitional movement

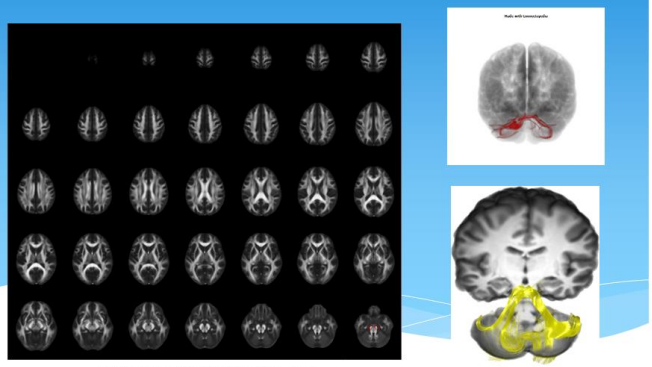

JHU atlas defined tract in red

Tract 2: Pontine Crossing Tract
Connects: Pons to contralateral cerebellum
Function: Coordination of movement

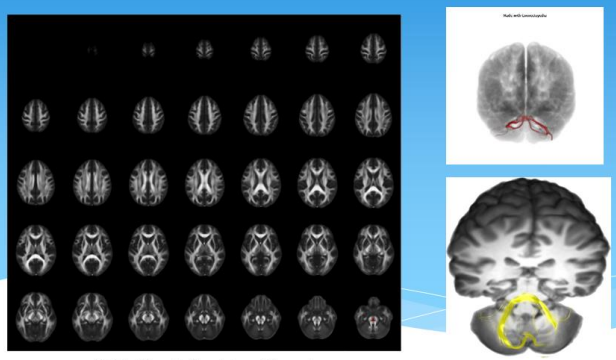

JHU atlas defined tract in red

Tract 3: Genu of the Corpus Callosum
Connects: Left and Right Anterior Frontal Lobes
Function: Interhemispheric coordination of executive functions

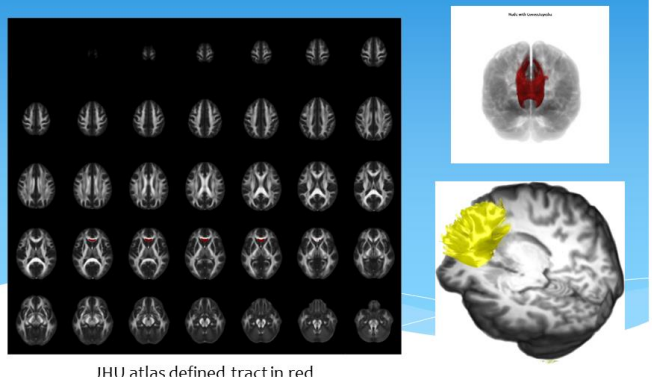

JHU atlas defined tract in red

Tract 4: Body of the Corpus Callosum
Connects: Left and Right Posterior Frontal Lobes and Left and Right Parietal Lobes
Function: Interhemispheric coordination of executive functions

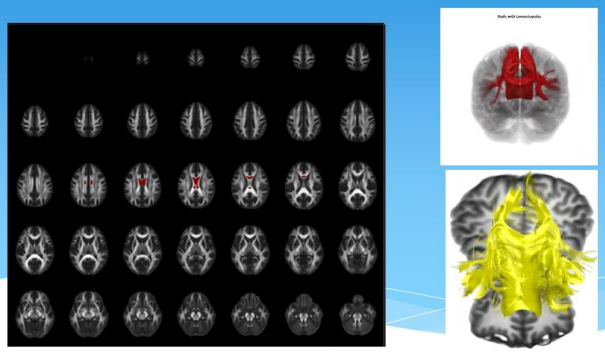

JHU atlas defined tract in red

Tract 5: Splenium of the Corpus Callosum
Connects: Left and Right Occipital Lobes
Function: Interhemispheric coordination of visual attention

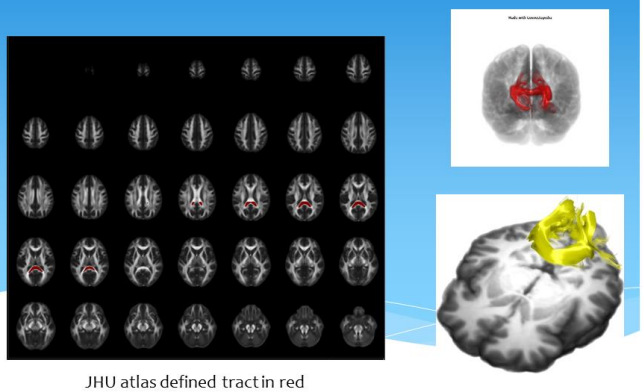

JHU atlas defined tract in red

Tract 6: Fornix
Connects: Hippocampus and mammillary bodies
Function: Short term memory

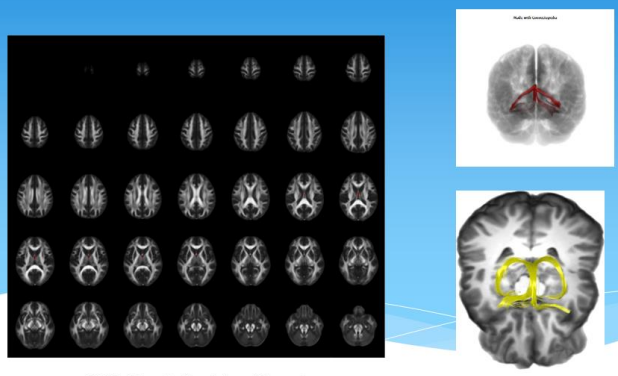

JHU atlas defined tract in red

THE CONCUSSION GROUP

MINDSET (QμANTify)

Tracts 7/8: R/L Corticospinal Tracts
Connects: Primary motor cortex with contralateral spinal motor neurons
Function: Motor control of contralateral side of the body

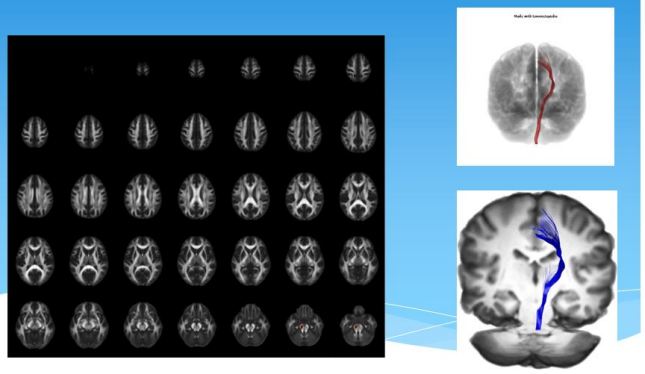

JHU atlas defined tract in red (showing rt hemisphere)

Tracts 9/10: R/L Medial Lemniscus
Connects: Dorsal Column Nuclei with Contralateral Thalamus (VPL)
Function: Somatosensory perception of contralateral side of the body

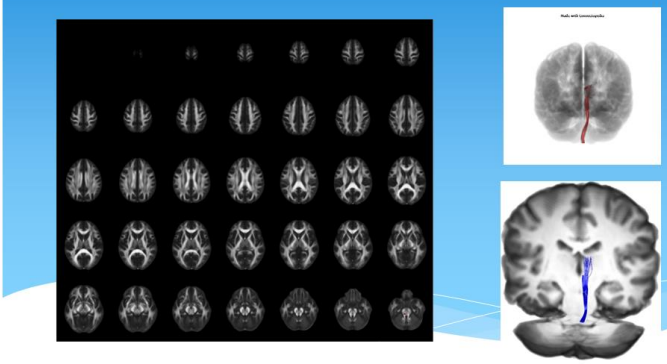

JHU atlas defined tract in red (showing rt hemisphere)

Tracts 11/12: R/L Inferior Cerebellar Peduncles
Connects: Connects spinal cord and medulla to cerebellum
Function: Supports posture, balance, coordination

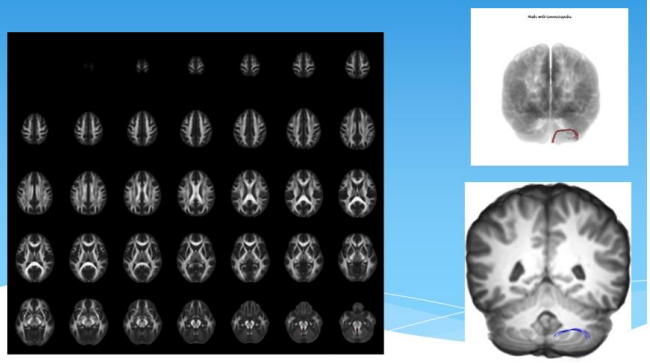

JHU atlas defined tract in red (showing rt hemisphere)

Tracts 13/14: R/L Superior Cerebellar Peduncles
Connects: Cerebellum to pons and midbrain
Function: Supports motor coordination and balance

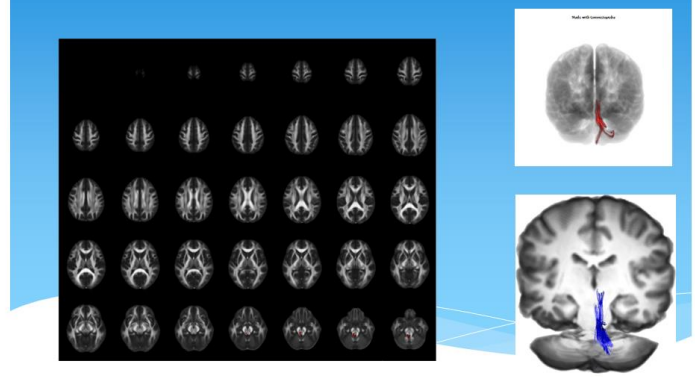

JHU atlas defined tract in red (showing rt hemisphere)

Tracts 15/16: R/L Cerebral Peduncles
Connects: Cerebellum with thalamus & motor cortex
Function: Motor control

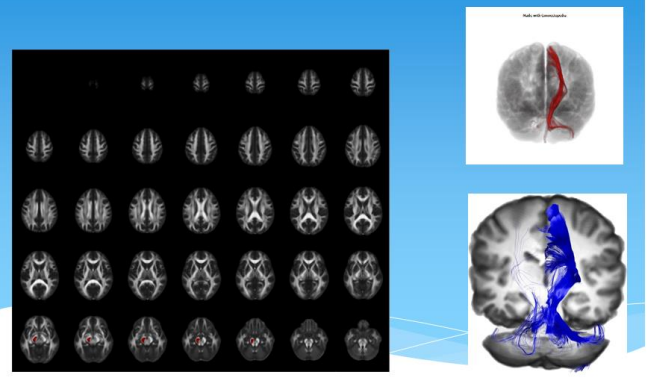

JHU atlas defined tract in red (showing rt hemisphere)

Tracts 19/20: R/L Posterior Limb of the Internal Capsule
Connects: Motor areas with brainstem; midbrain and occipital lobe; midbrain to thalamus and temporal lobe
Function: Supports somato-motor, auditory, and visual functions

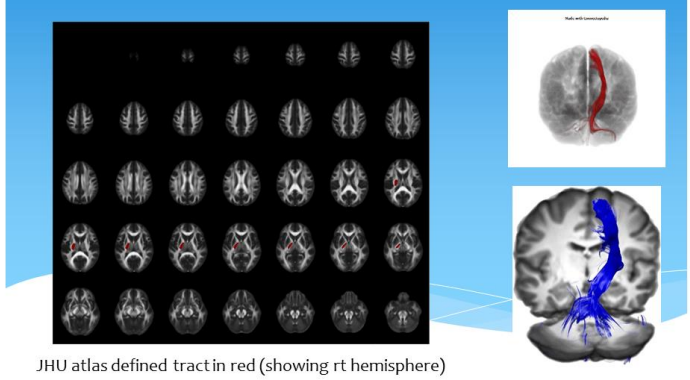

JHU atlas defined tract in red (showing rt hemisphere)

Tracts 21/22: R/L Retrolenticular Part of the Internal Capsule
Connects: Thalamus and occipital cortex
Function: Vision

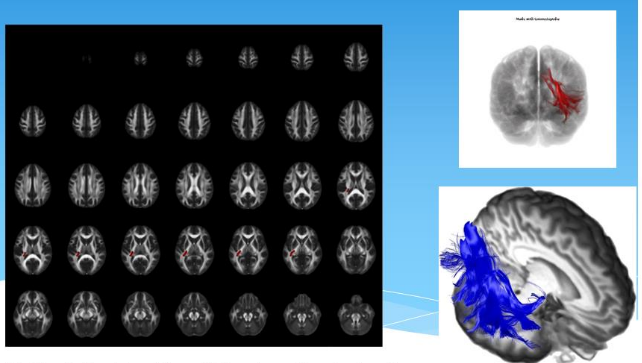

JHU atlas defined tract in red (showing rt hemisphere)

Tracts 23/24: R/L Anterior Corona Radiata
Connects: Descending and ascending fibers related to cortex, especially frontal lobes
Function: Higher cognitive functioning

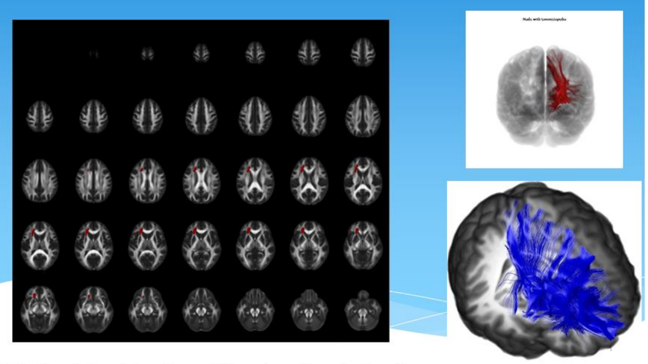

JHU atlas defined tract in red (showing rt hemisphere)

Tracts 25/26: R/L Superior Corona Radiata
Connects: Ascending and descending fibers for motor cortical regions
Function: Supports motor control

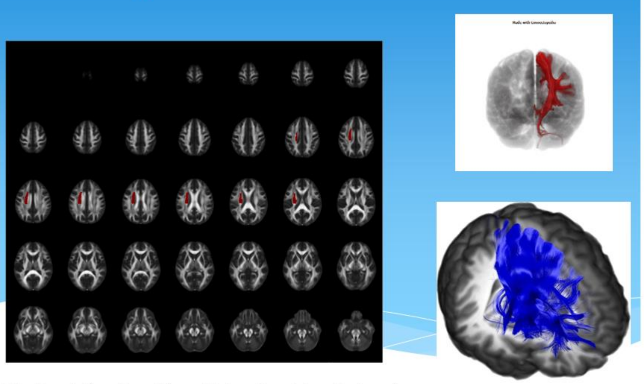

JHU atlas defined tract in red (showing rt hemisphere)

Tracts 27/28: R/L Posterior Corona Radiata
Connects: Ascending and descending fibers for parietal cortex
Function: Supports attentional control, somatosensory function

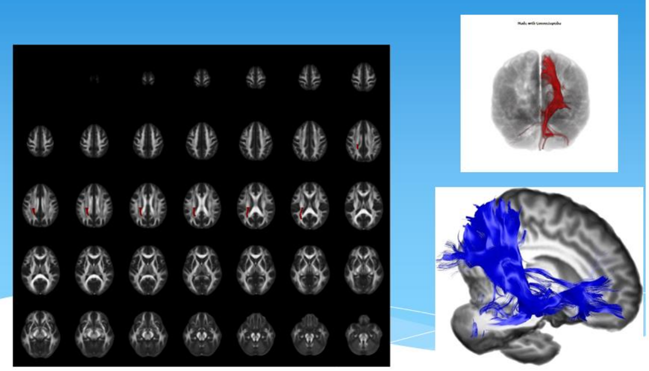

JHU atlas defined tract in red (showing rt hemisphere)

Tracts 29/30: R/L Posterior Thalamic Radiation
Connects: Thalamus and cortex
Function: Visual and auditory function

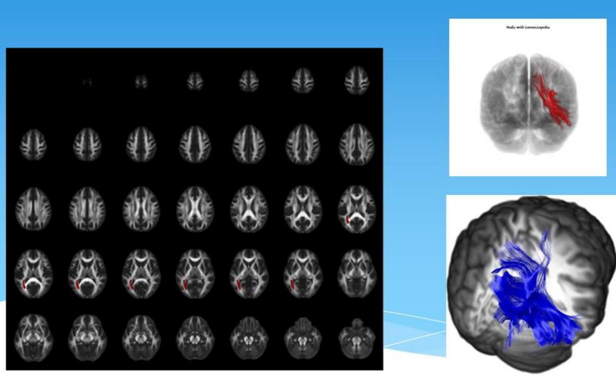

JHU atlas defined tract in red (showing rt hemisphere)

Tracts 31/32: R/L Sagittal Stratum
Connects: Thalamus and occipital, parietal, temporal and cingulate cortex
Function: Visual , auditory, cognitive function

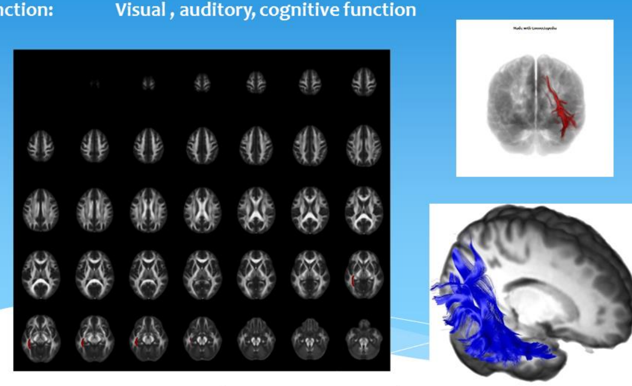

JHU atlas defined tract in red (showing rt hemisphere)

THE CONCUSSION GROUP

MINDSET (Quantify)

Tracts 33/34: R/L External Capsule
Connects: Cortico-cortical association fibers for occipital, temporal, parietal and cingulate cortex
Function: Supports cognitive processing

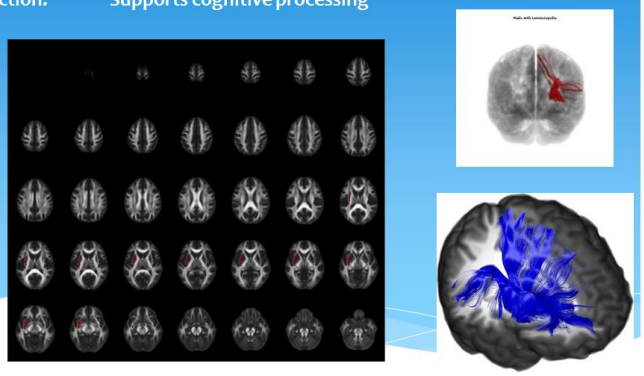

JHU atlas defined tract in red (showing rt hemisphere)

Tracts 35/36: R/L Cingulum (cingulate gyrus)
Connects: Prefrontal cortex and cingulate
Function: Supports cognitive cognitive, decision making

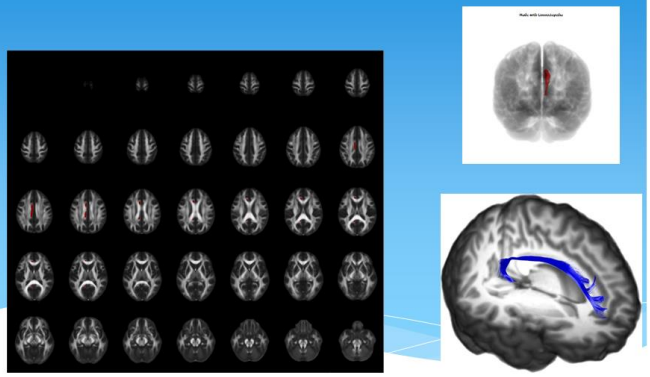

JHU atlas defined tract in red (showing rt hemisphere)

Tracts 37/38: R/L Cingulum (hippocampus)
Connects: Cingulate and entorhinal cortex
Function: Memory, emotional processing

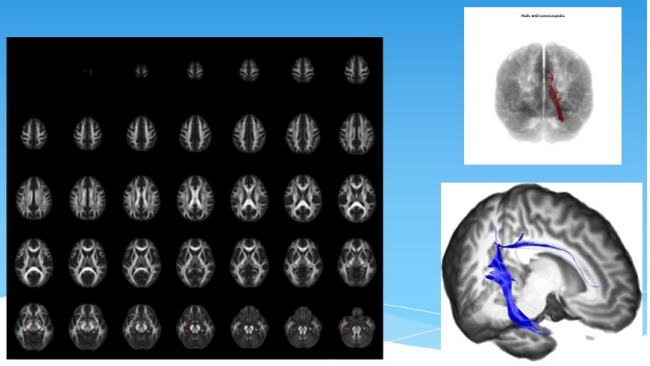

JHU atlas defined tract in red (showing rt hemisphere)

Tracts 39/40: R/L Fornix (cres) and stria terminalis
Connects: Hippocampus and mammillary bodies; amygdala with the septal region and hypothalamus
Function: Memory, emotional processing, fear response

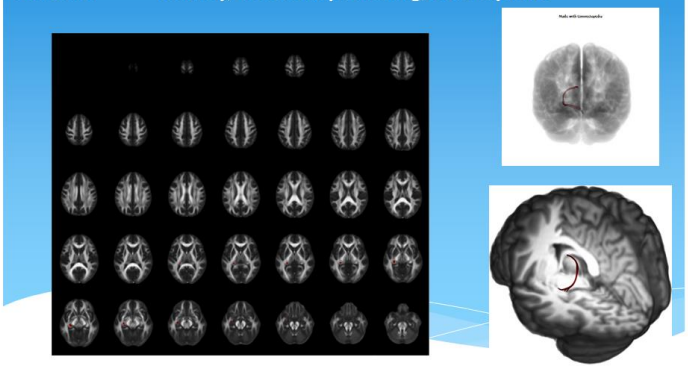

JHU atlas defined tract in red (showing rt hemisphere)

Tracts 41/42: R/L Superior Longitudinal Fasciculus
Connects: Interconnects front and back of cerebrum including frontal, parietal, occipital and cingulate areas
Function: Higher cortical functions

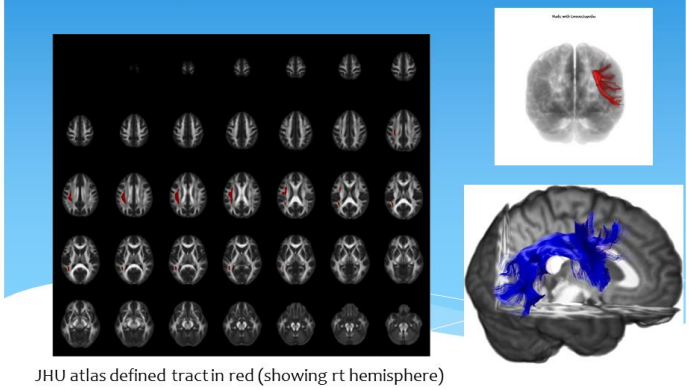

JHU atlas defined tract in red (showing rt hemisphere)

Tracts 43/44: R/L Superior Fronto-Occipital Fasciculus
Connects: Interconnects frontal lobe with the occipital & parietal lobes
Function: Spatial awareness

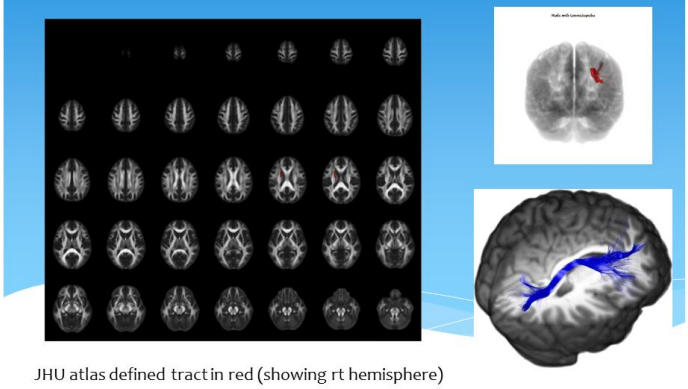

JHU atlas defined tract in red (showing rt hemisphere)

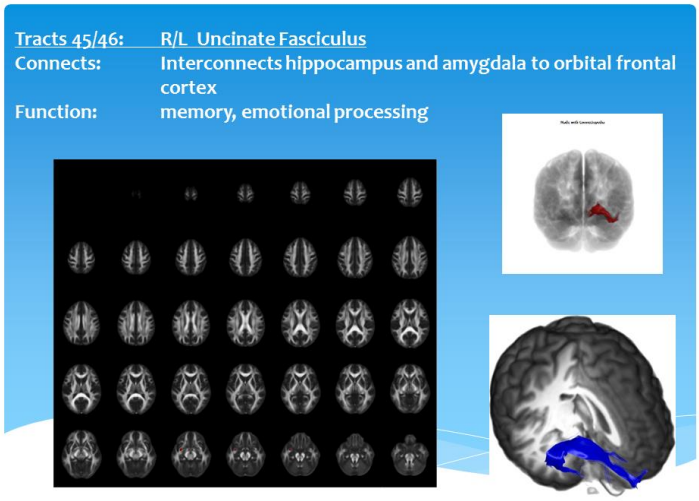

JHU atlas defined tract in red (showing rt hemisphere)

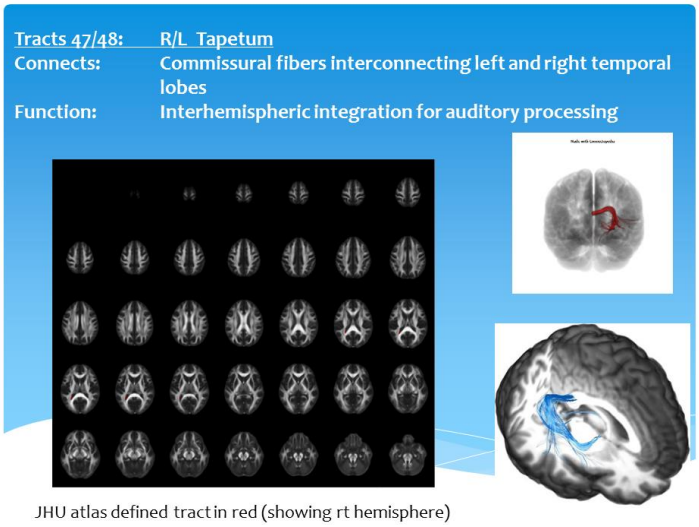

JHU atlas defined tract in red (showing rt hemisphere)

MRI in Traumatic Brain Injury (TBI) and Concussion

As mentioned, it is not uncommon for routine clinical MRI to be interpreted as within normal limits following TBI. Indeed, gross structural abnormalities on visual inspection are seen in less than 20% of cases. However, using quantitative volumetric and DTI analyses, sensitivity is increased to >50%.

A number of studies report TBI related reductions in regional brain volumes (e.g., Bigler et al., 1997; Bendlin et al., 2008; Spitz et al., 2013). Traumatic brain injury is a process, not an event, with secondary injury cascades extending for the minutes, hours, days, months and years following the initial traumatic event. When present, volume reductions may be focal to regions at coup and counter coup locations, or they may manifest diffusely with cortical atrophy and/or expansion of the ventricles (Bigler et al., 1997; MacKenzie et al., 2002).

Hippocampal atrophy is also a common consequence of TBI. Animal studies indicate that a very rapid loss of cells within the CA3 region of the hippocampus can be seen following a cortical contusion (Baldwin et al., 1997), with continued loss of cortical tissue, shrinkage of the hippocampal pyramidal cell layer, and reactive astrocytosis continuing for at least one year following TBI (Smith et al., 1997). Similar observations have been made in human studies, with evidence of progressive cortical and hippocampal atrophy following even mild TBI (Bigler et al, 1997; MacKenzie et al., 2002; Beauchamp et al., 2010; Bigler and Maxwell, 2011; Ross et al., 2013; Zhou et al., 2013).

It should also be noted that some recent studies demonstrate that increased cortical thickness (Wang et al, 2015) and increased regional brain volumes (e.g., Ross et al., 2019) may also be seen following TBI, most likely in relationship to edema, chronic neuro-inflammation, or compensatory mechanisms.

Dozens of human and animal studies indicate that even mild head trauma can cause a significant disruption in the integrity of white matter pathways as assessed via histopathology in animal studies and diffusion tensor imaging in human cases. Recent reviews (Hulkower et al., 2013; Wilde et al., 2015; Khong et al., 2016) all conclude that there is substantial evidence and agreement among researchers that TBI is most commonly

associated with reduced FA values during the chronic phase of injury, with the corpus callosum often implicated. In the sub-acute phase after injury there may be findings of increased FA values. Increased FA following injury is thought to reflect intracellular swelling, reactive astrogliosis, compaction of neurofilament, infiltration of inflammatory cells into the extracellular space, loss of crossing fibers and/or reorganization in response to injuries in other areas (Croall et al., 2014). In some cases, increased FA can persist into the chronic period (Dennis et al., 2018). Regardless, there is strong evidence that DTI methods are viable for detecting TBI related axonal injury and both group and individual subject levels (using quantitative large database approaches). DTI is increasingly being used in a medical-legal context, and despite occasional Daubert challenges, properly performed DTI has always been admitted in civil and criminal cases.

References

Baldwin SA, Gibson T, Callihan CT, Sullivan PG, Palmer E, Scheff SW. (1997) Neuronal cell loss in the CA3 subfield of the hippocampus following cortical contusion utilizing the optical dissection method for cell counting. J Neurotrauma 14:385-398.

Beauchamp MH, Ditchfield M, Maller JJ, Catroppa C, Godfrey C, Rosenfeld JV, Kean MJ, Anderson VA. (2010) Hippocampus, amygdala and global brain changes 10 years after childhood traumatic brain injury. Int J Dev Neurosci 30:217-224.

Bendlin BB, Ries ML, Lazar M, Alexander AL, Dempsey RJ, Rowley HA, Sherman JE, Johnson SC. (2008) Longitudinal changes in patients with traumatic brain injury assessed by diffusion-tensor and volumetric imaging. Neuroimage 42:503-514,

Bigler ED, Blatter DD, Anderson CV, Johnston SC, Gale SD, Hopkins RO, Burnett B. (1997) Hippocampal volume in normal aging and truamtic brain injury. AJNR Am J Neuroradiol 18: 11-23.

Bigler ED, Maxwell WM. (2011) Neuroimaging and neuropathology of TBI. Neurorehabilitation 28: 63.74.

Croall ID, Cowie CJ, Je J, Peel Am Wood J, Aribisala BS, Mitchell P, Mendelow D, Smith FE, Miller D, Kelly T, Blamire AM. (2014) White matter correlates of cognitive dysfunction after mild traumatic brain injury. Neurology 83: 494-501.

Dennis EL, Wilde EA, Newsome MR, Scheibel RS, Troyanskaya M, Velez C, et al., (2018) ENIGMA military brain injury: a coordinated meta-analysis of diffusion MRI from multiple cohorts. Poc IEEE Int Symp Biomed Imaging. Apr 2018: 1386-1389.

Hulkower MB, Poliak DB, Rosenbaum SB, Zimmerman ME, Lipton ML. (2013) A decade of DTI in traumatic brain injury: 10 years and 100 articles later. AJNR Am J Neuroradiol 34: 2064-2074.

Khong E, Odenwald N, Hashim Em Cusimano MD. (2016) Diffusion tensor imaging findings in post-concussive syndrome patients after mild traumatic brain injury: A systematic review. Front Neurol 19: 156

Lancaster JL, Woldorff MG, Parsons LM, Liotti M, Freitas CS, Rainey L, Kochunov PV, Nickerson D, Mikiten SA, Fox PT. (2000) Automated Talairach atlas labels for functional brain mapping. Hum Brain Mapp 10:120–131.

MacKenzie JD, Siddiqi F, Babb JS, Bagley LJ, Mannon LJ, Sinson GP, Grossman RI. (2002) Brain atrophy in mild or moderate traumatic brain injury: a longitudinal quantitative analysis. AJNR Am J Neuroradiol 23: 1509-1515.

Mori S, Oishi K, Faria AV. (2009) White matter atlases based on diffusion tensor imaging. Curr Opn Neurol 22(4): 362-339.

Palacios EM, Martin AJ, Boss MA, Ezekiel F, Chang YS, Yuh EL, Vassar MJ, Schnyer DM, MacDonald CL,

Crawford KL, Irimia A, Toga AW, Mukherjee, and Track-TBI Investigators. Toward precision and reproducibility of diffusion tensor imaging: A multicenter diffusion phantom and traveling volunteer study. AJNR Am J Neuroradiol 38:537-545.

Ross DE, Ochs AL, Seabaugh JM, Shrader CR; ADNI. (2013) Man versus machine: comparison of radiologists; interpretations and NeuroQuant volumetric analysis of brain MRIs in patients with traumatic brain injury. J Neuropsychiatry Clin Neurosci 25: 32-39.

Ross DE, Seabuagh JD, Seabaugh JM, Alvarez C, Peyton Ellis L, Powell C, Hall C, Reese C, Cooper L, Ochs AL. (2019) Patients with chronic mild or moderate traumatic brain injury have abnormal brain enlargement. Brain Inj, Sept 2019, epub ahead of print.

Smith DH, Chen XH, Pierce JE, Wolf JA, Trojanowski JQ, Graham DI, McIntosh TK. (1997) Progressive atrophy and neuronal death for one year following traumatic brain injury in the rat. J Neurotrauma 14:715-727.

Spitz G, Bigler ED, Abildskov T, Maller JJ, O'Sulivan R, Ponsford JL. (2013) Regional cortical volume and cognitive function following traumatic injury. Brain Cogn 83:34-44.

Tzourio-Mazoyer N, Landeau B, Papathanassiou D, Crivello F, Etard O, Delcroix N, Mazoyer B, Joliot M. (2002) Automated anatomical labeling of activations in SPM using a macroscopic anatomical parcellation of the MNI MRI single-subject brain. Neuroimage 15(1): 273-289.

Venkatraman VK, Gonzalez CE, Landman B, Goh J, Reiter DA, An Y, Resnick SM. (2015) Region of interest correction factors improve reliability of diffusion imaging measures within and across scanners and field strengths.

Wang X, Xie H, Cotton A, Tamburrino M, Brickman K, Lewis T, McLean S, Liberzon I. (2015) Early cortical t hickness change after mild traumatic brain injury following motor vehicle collision. J Neutotrauma 32:455-463.

Wilde EA, Bouix S, Tate DF, Lin AP, Newsome MR, Taylor BA, Stone JR, Montier J, Gandy SE, Biekman B, Shenton ME, York G. (2015) Advanced neuroimaging applied to veterans and service personnel with traumatic brain injury: state of the art and potential benefits. Brain Imaging Behav 9: 367-402.

Zhou Y, Kierans A, Kenul D, Ge Y, Rath J, Reaume J, Grossman RI, Lui YW. (2013) Mild traumatic brain injury: longitudinal regional brain volume changes. Radiology 267: 88-890.

Additional litigation services available through our network of experts

- DTI Education
- Expert Identification and Management
- Legal Expertise
- Complex Case Approach
- Trial Preparation
- Court Friendly Visual Aids - including 3D Exhibits

Team Members

Edward Soll, M.D.	Medical Director and Litigation Consultant
Jeffrey Lewine, Ph.D.	Neuroscientific Coordinator
Anne Foundas, M.D., FAAN	Cognitive Neurology Physician
Maury Herman, J.D.	Corporate Advisor
Shea Soll, M.B.A.	Director of Business Development and Corporate Partnerships

www.theconcussiongroup.com
888.214.2095